This is a preprint, the final version is subject to change, of the American Mineralogist (MSA)
Cite as Authors (Year) Title. American Mineralogist, in press.
DOI: https://doi.org/10.2138/am-2019-6735

(Revision 2)

The quench control of water estimates in convergent margin magmas

(Revision 2)

Maxim Gavrilenko[1,2], Michael Krawczynski[1], Philipp Ruprecht[2], Wenlu Li[3], Jeffrey G. Catalano[1]

[1]Department of Earth and Planetary Sciences, Washington University in St. Louis, Campus Box 1190, One Brookings Drive, St. Louis, MO 63130, United States

[2]Department of Geological Science and Engineering, University of Nevada, Reno, 1664 N. Virginia Street, Reno, NV 89557, United States

[3]Department of Energy, Environmental, and Chemical Engineering, Washington University in St. Louis, Campus Box 1180, One Brookings Drive, St. Louis, MO 63130, United States

Abstract

Here we present a study on the quenchability of hydrous mafic melts. We show via hydrothermal experiments that the ability to quench a mafic hydrous melt to a homogeneous glass at cooling rates relevant to natural samples has a limit of no more than 9 ±1 wt% of dissolved H_2O in the melt. We performed supra-liquidus experiments on a mafic starting composition at 1-1.5 GPa spanning H_2O undersaturated to H_2O saturated conditions (from ~1 wt% to ~21 wt%). After dissolving H_2O and equilibrating, the hydrous mafic melt experiments were quenched. Quenching rates of 20 to 90 K/s at the glass transition temperature were achieved and some experiments were allowed to decompress from thermal contraction while others were held at an isobaric condition during quench. We found that quenching of a hydrous melt to a homogeneous glass at

Always consult and cite the final, published document. See http:/www.minsocam.org or GeoscienceWorld

This is a preprint, the final version is subject to change, of the American Mineralogist (MSA)
Cite as Authors (Year) Title. American Mineralogist, in press.
DOI: https://doi.org/10.2138/am-2019-6735

quench rates comparable to natural conditions is possible at water contents up to 6 wt%. Melts containing 6-9 wt% of H_2O are partially quenched to a glass, always containing significant fractions of quench crystals and glass alteration/devitrification products. Experiments with water contents greater than 9 wt% have no optically clear glass after quench and result in fine-grained mixtures of alteration/devitrification products (minerals and amorphous materials). Our limit of 9 ±1 wt% agrees well with the maximum of dissolved H_2O contents found in natural glassy melt inclusions (8.5 wt% of H_2O). Other techniques for estimating pre-eruptive dissolved H_2O content using petrologic and geochemical modeling have been used to argue that some arc magmas are as hydrous as 16 wt% of H_2O. Thus, our results raise the question whether the observed record of glassy melt inclusions has an upper limit that is partially controlled by the quenching process. This potentially leads to underestimating the maximum amount of H_2O recycled at arcs when results from glassy melt inclusions are predominantly used to estimate water fluxes from the mantle.

Keywords: mafic glassy melt inclusions, hydrous mafic glass quenchability, arc volatile budget, magmatic water

Introduction

Arc magmas are almost exclusively hydrous (e.g. Wallace 2005; Métrich and Wallace 2008; Plank et al. 2013; Zellmer et al. 2015) as a result of subducting slab dehydration (Grove et al. 2006). The maximum dissolved H_2O content in magmas plays a pivotal role in the generation (Katz et al. 2003; Grove et al. 2006; Grove et al. 2012), and

Always consult and cite the final, published document. See http:/www.minsocam.org or GeoscienceWorld

This is a preprint, the final version is subject to change, of the American Mineralogist (MSA)
Cite as Authors (Year) Title. American Mineralogist, in press.
DOI: https://doi.org/10.2138/am-2019-6735

evolution (Grove et al. 2003; Zimmer et al. 2010; Grove et al. 2012) of arc melts. Within the crust, magma transport and eruption is strongly modulated by dissolved H_2O since it imparts buoyancy to primitive magmas traveling through the crust (Herzberg et al. 1983; Ochs and Lange 1999; Carmichael 2002), and when H_2O exsolves at shallow pressures, it affects explosivity through volumetric expansion (Cashman 2004). Besides the effects of H_2O on the magmatic system itself, the H_2O budget in convergent margins affects mantle rheology and geophysical parameters like seismic wave speed, attenuation, and conductivity of the lithosphere and mantle (Hacker et al. 2003; Pozgay et al. 2009; McGary et al. 2014). Because water plays such a central role in magma genesis and evolution at convergent margins, knowing the water content of the most primitive magma samples at volcanic arcs is of first order importance.

Currently, magmatic H_2O content estimations are based mostly on studies of melt inclusions (e.g. Frezzotti 2001; Danyushevsky et al. 2002; Schiano 2003; Kent 2008); in particular melt inclusions that are glassy and hosted by the most magnesian olivine crystals, present in tephra/scoria. Melt inclusions (MIs) act as tiny pressure capsules potentially preserving the chemistry of pristine primitive melts as well as minimum dissolved H_2O contents. The physical state of a MI post entrapment can be thought of as having three major end-members: 1) *glassy* MIs; 2) *crystallized* MIs 3) *devitrified* MIs. The resulting type of the MI strongly depends on its cooling rates (Frezzotti 2001). Because it has long been assumed that the glassy single-phase melt inclusions have the most rapid cooling rates, direct SIMS (Secondary Ion Mass Spectrometer) and FTIR (Fourier-Transform Infrared Spectroscopy) measurements of H_2O dissolved in *glassy* MIs have served for decades as the 'gold standard' for determining magmatic pre-

Always consult and cite the final, published document. See http:/www.minsocam.org or GeoscienceWorld

This is a preprint, the final version is subject to change, of the American Mineralogist (MSA)
Cite as Authors (Year) Title. American Mineralogist, in press.
DOI: https://doi.org/10.2138/am-2019-6735

eruptive H_2O content (e.g. Wallace 2005; Plank et al. 2013). C*rystallized* MIs are thought to be produced in slowly cooling conditions (Frezzotti 2001) and thus are usually presumed to be subject to diffusive degassing of H_2O in nature. These inclusions are rarely used for volatile species studies (e.g. Esposito et al. 2016). *Devitrified* MIs are results from partial modifications of the glass; and those melt inclusions are usually discarded by researchers of magmatic volatile species (Kent 2008).

While the evolution of magmatic H_2O at shallow depths has been studied thoroughly using glassy MI (e.g. Wallace 2005; Plank et al. 2013), the evolution of magmatic H_2O in deeper parts of subduction zones remains less constrained. Volatile-rich magmas undergo nearly complete degassing during ascent, eruption, and cooling. Because H_2O solubility is pressure dependent (e.g. Moore et al. 1998; Papale et al. 2006; Shishkina et al. 2010; Mitchell et al. 2017), high water contents above 9 wt% would require MIs formed at mid to lower crustal or even upper mantle pressures, but no glassy melt inclusions preserving >9 wt.% H_2O have been found. The existence and preservation of such melt inclusions is further challenged by the fact that hydrogen diffusion through the crystal lattice of the host allows equilibration between the degassing matrix melt and the entrapped pressurized melt droplet. Recent studies have demonstrated that hydrogen diffusion within a host mineral is rapid (Danyushevsky et al. 2002; Hauri 2002; Portnyagin et al. 2008; Chen et al. 2011; Gaetani et al. 2012; Bucholz et al. 2013; Lloyd et al. 2013; Hartley et al. 2015) causing MIs to be partially open to lose (or gain) volatile species. Hydrogen may also migrate along dislocations or propagation of defect points in the host mineral (Massare et al. 2002; Portnyagin et al. 2008) further enhancing hydrogen exchange between the melt inclusion and the matrix melt. Thus, it has been

Always consult and cite the final, published document. See http:/www.minsocam.org or GeoscienceWorld

This is a preprint, the final version is subject to change, of the American Mineralogist (MSA)
Cite as Authors (Year) Title. American Mineralogist, in press.
DOI: https://doi.org/10.2138/am-2019-6735

93 acknowledged that the amount of H_2O MIs contain likely represents a minimum from
94 what was originally dissolved in a particular magma (Gaetani and Watson 2000;
95 Danyushevsky et al. 2002; Hauri 2002; Portnyagin et al. 2008; Gaetani et al. 2012;
96 Bucholz et al. 2013; Lloyd et al. 2013).

97 Despite the limitations in the use of glassy melt inclusions they are still assumed
98 to be among the best archives to record pre-eruptive primitive water contents (e.g.
99 Wallace 2005; Plank et al. 2013; Wallace et al. 2015b), especially when quenched rapidly
100 as tephra of mafic magmas. The rapid quench of the melt inclusions upon eruption or
101 even before eruption results in the preservation of the melt inside host minerals as clear
102 glass. By preferentially analyzing samples from primitive olivine phenocrysts in tephra
103 and scoria, it is assumed that these samples represent the best estimates for pre-eruptive
104 water contents of melts that originate in the mantle. The highest amount of water
105 recorded in melt inclusions with mafic compositions is ~8.5 wt% (de Moor et al. 2013)
106 hosted in minerals from nephelinitic magmas, related to the rift settings. In arc settings
107 the maximum is slightly lower at 7.0-7.5 wt% of H_2O (Auer et al. 2009; Zimmer et al.
108 2010; Weller and Stern 2018).

109 Many excellent MI studies have significantly improved our understanding of the
110 H_2O variations in arc magmas (e.g. review/summary in Wallace 2005; Kent 2008; Plank
111 et al. 2013). A review of the existing database of inclusions that have been quantitatively
112 studied for their dissolved H_2O contents concluded that the maximum H_2O content in
113 melt inclusions from a single volcano or cinder cone ranges typically between 1-7 wt%
114 (Plank et al. 2013). Those researchers (Plank et al. 2013) and other studies (Gaetani and
115 Watson 2000; Danyushevsky et al. 2002; Hauri 2002; Portnyagin et al. 2008; Gaetani et

Always consult and cite the final, published document. See http:/www.minsocam.org or GeoscienceWorld

This is a preprint, the final version is subject to change, of the American Mineralogist (MSA)
Cite as Authors (Year) Title. American Mineralogist, in press.
DOI: https://doi.org/10.2138/am-2019-6735

al. 2012; Bucholz et al. 2013; Lloyd et al. 2013) have recognized the open system behavior of MIs. Nonetheless, it is still generally interpreted that the maximum water contents of MIs in primitive magmas in subduction zone settings are representative of the amount of H_2O in primitive arc melts (e.g. Straub and Layne 2003; Wallace 2005; Moore 2008; Parai and Mukhopadhyay 2012; Wallace et al. 2015b; Peslier et al. 2017).

An alternative interpretation of the maximum water content found in glassy melt inclusions is that melts with higher water contents do not quench to a homogeneous glass at natural quenching rates. Such higher water contents (14-16 wt%) for arc magmas have been postulated based on other petrologic constraints to exist at deep crust and upper mantle conditions (Carmichael 2002; Fischer and Marty 2005; Krawczynski et al. 2012). The fact that the majority (98%) of studied glassy MIs record last equilibration at shallow pressures (< 500 MPa; Wallace 2005) raises the question whether all MIs formed and/or equilibrated at shallow depths or whether MIs are formed at all pressures, but by selectively analyzing glassy samples there is a bias in the current data set to low H_2O melt inclusions or those that formed or re-equilibrated shallowly. Here we show that the low pressure record in MIs is not only a result of shallow entrapment or re-equilibration on ascent, but potentially also due to the ability of quenched glass to retain H_2O in its structure when it is formed as the hydrous silicate melt passes the glass transition.

Here we define the term "quenchability", which refers to the ability of a silicate melt to be transformed to a glass upon cooling. This kinetically driven process strongly depends on such parameters as melt polymerization degree and cooling rates (Dingwell and Webb 1990). Adding a significant amount of H_2O to a melt lowers the glass transition temperature (Tg), potentially making hydrous melts harder to quench and

Always consult and cite the final, published document. See http:/www.minsocam.org or GeoscienceWorld

This is a preprint, the final version is subject to change, of the American Mineralogist (MSA)
Cite as Authors (Year) Title. American Mineralogist, in press.
DOI: https://doi.org/10.2138/am-2019-6735

139 producing *non-glassy* melt inclusions. Devitrified or crystallized MIs are preferentially
140 not studied for their volatile content. Below we present evidence that if hydrous magmas
141 contain greater than ~9 wt% H_2O they cannot form glassy MIs at naturally occurring
142 quench rates. Studies that make global calculations of water exchange between the
143 Earth's interior and the exosphere using MI data for estimates of H_2O contents in arc
144 magmas (e.g. Hacker 2008; van Keken et al. 2011; Parai and Mukhopadhyay 2012), are
145 likely underestimating the amount of recycled H_2O in some sub-arc settings. In addition
146 recent geophysical studies show that the amount of subducted water may be much higher
147 than previously realized (Cai et al. 2018), which would require some amount of arc
148 magmas to contain higher water contents than traditionally recognized.
149

150 **Experimental approach**

151 The MI record stands in contrast to studies using petrologic and geochemical
152 proxies that provide evidence for up to 16 wt% of H_2O in some arc magmas (Carmichael
153 2002; Fischer and Marty 2005; Krawczynski et al. 2012). An underlying assumption in
154 MI studies is that glassy MIs (single phase ± a single exsolution bubble) have the best
155 chance to faithfully record pre-eruptive H_2O content, while non-glassy MIs (multiple
156 phases) are commonly interpreted as potentially slowly cooled (and, thus, have
157 experienced more H_2O degassing by diffusion) and also require additional stages of
158 sample preparation (e.g. Esposito et al. 2016). Anecdotally, many previous experimental
159 studies involving H_2O bearing silicate melts have reported problems with quenching
160 mafic glasses with high water content of more than 8 wt% of H_2O (e.g. Grove et al. 2006;
161 Behrens et al. 2009; Baker and Alletti 2012; Shishkina 2012). However, the

Always consult and cite the final, published document. See http:/www.minsocam.org or GeoscienceWorld

quenchability limit for hydrous silicate melts has not been studied systematically before. Thus, how much water can we quench in a single-phase glassy inclusion with naturally occurring cooling rates?

To test the limits of quenchability for hydrous glasses for naturally occurring cooling rates, we conducted a series of hydrous (1-21 wt% of pre-loaded H_2O) supra-liquidus temperature experiments (1225-1300^{o}C, 1-1.5 GPa) on a mafic calc-alkaline composition (Table 1), in order to determine the highest concentration of dissolved H_2O_{total} that a quenched glass is able to contain (H_2O_{total} accounts for all hydrogen species in the glass). The mafic composition for experiments was chosen because previous studies that explore primitive magma water contents are in the mafic range of 44-56 wt% of SiO_2 (Fig. 1). Synthetic glass powders and deionized water were loaded in $Au_{80}Pd_{20}$ metal capsules and heated above the liquidus and equilibrated for 10-16 hours in a piston-cylinder apparatus. The experiments were heated to 1225-1300^{o}C, near or above the liquidus (depending on the water content), and quenched at rates applicable to cooling rates for volcanic tephra (Lloyd et al. 2013) (see Materials and Methods section for more details). Dissolved H_2O contents in quenched experimental run products were determined by thermo-gravimetric analysis (TGA), electron microprobe analysis (EPMA; "volatiles by difference" method), and secondary ion mass spectrometry SIMS.

The experimental pressure (1-1.5 GPa) represents deep crustal and shallow mantle pressures. We have chosen this pressure because H_2O solubility in the melt is sufficiently high (~16-20 wt% H_2O; e.g. Shishkina et al. 2014; Mitchell et al. 2017 and references therein) to contain far more dissolved H_2O than what is recorded in natural glassy MIs. Overall, H_2O solubility in melts/glasses of different compositions has been best

Always consult and cite the final, published document. See http:/www.minsocam.org or GeoscienceWorld

This is a preprint, the final version is subject to change, of the American Mineralogist (MSA)
Cite as Authors (Year) Title. American Mineralogist, in press.
DOI: https://doi.org/10.2138/am-2019-6735

constrained at conditions <500 MPa representing crustal depths shallower than 15-16 km (Hamilton et al. 1964; Moore et al. 1998; Papale et al. 2006; Shishkina et al. 2010 and others).

Materials and Methods

Starting materials

Experiments were conducted on a starting composition that was synthesized to match the composition of a primitive basaltic andesite (Mg#=71), 85-44, erupted from Mt. Shasta, CA, in the Cascades (Baker et al. 1994; Grove et al. 2003, 2005). This basaltic andesite was chosen because it is a low silica (52 wt% SiO_2), high-MgO (10.5 wt% MgO) end member of the Mt. Shasta primitive lava suite, and known from experimental studies to be a hydrous magma composition. The starting composition was made from reagent grade oxides and carbonates, ground under isopropanol in a ball mill, and decarbonated at 1000°C for 8 hours. The ground powder was glassed at 1,500°C in a Pt crucible in air for 1 hour, and then quenched in the crucible by dropping it in water. The glass was extracted from the crucible and ground in an agate mortar under isopropanol. The ground glass was then remelted in air and quenched and crushed following the same procedures to ensure homogeneity. In total, the melting/grinding procedure was repeated three times to ensure homogeneous and crystal free starting material. The major element composition and homogeneity of the glass starting material was inspected by electron microprobe analysis (Table 1).

Since the starting material was glassed in air we expect the starting material to have all iron as Fe^{3+}, before the experiments. However, the experiments (see below for

Always consult and cite the final, published document. See http:/www.minsocam.org or GeoscienceWorld

This is a preprint, the final version is subject to change, of the American Mineralogist (MSA)
Cite as Authors (Year) Title. American Mineralogist, in press.
DOI: https://doi.org/10.2138/am-2019-6735

procedures) were unbuffered for fO_2 (oxygen fugacity). The presence of Fe-bearing olivine and orthopyroxene crystals in some of the experimental products (Table 2, 3) confirms that some of the Fe^{3+} was reduced to Fe^{2+} during the experiments. It was shown recently that increasing Fe^{3+} content of anhydrous silicate melts increases their viscosity and glass transition temperature (Di Genova et al. 2017), which indirectly means that increasing Fe^{3+} improves the quenchability. The effect of fO_2 on hydrous glasses quenchability has not yet been studied directly. In our case we expect the Fe^{3+}/Fe^{2+} to be higher than zero, but at this time it is unconstrained.

Experimental procedures

Experiments were conducted using the 1/2 piston cylinder apparatus (Boyd and England 1960) at the Washington University Experimental Studies of Planetary Materials laboratory. We employed a single capsule, which contains an unbuffered mixture of powdered glass starting material and deionized water. We used an $Au_{80}Pd_{20}$ alloy capsule for all experiments. The capsule was prepared with a small lip and is fitted with a lid that is cold-welded by pressure (Ayers et al. 1992), a design that has been successful in super-hydrous experiments (e.g. Brenan et al. 1994; Brenan et al. 1995; Krawczynski et al. 2012). The lid seals when the piston load is applied to the capsule during pressurization, before heating. The capsule is surrounded by a soft-fired pyrophyllite ring. During compression the pyrophyllite ring deforms with the capsule and helps avoid any shear stresses from developing. A $BaCO_3$ pressure cell was used in all experiments. Most of the experiments were conducted on glass starting materials at 1 GPa, but several experiments were conducted at 1.5 GPa (see details below). Experiments were doped with different

Always consult and cite the final, published document. See http:/www.minsocam.org or GeoscienceWorld

This is a preprint, the final version is subject to change, of the American Mineralogist (MSA)
Cite as Authors (Year) Title. American Mineralogist, in press.
DOI: https://doi.org/10.2138/am-2019-6735

231 starting amounts of deionized water ranging from ~1% to ~21% of the weight of sample
232 glass + H_2O (Table 2). Turning off the power quenched the experiments. Cooling during
233 the finite quench duration leads to thermal contraction and a concurrent drop of pressure
234 on the sample (Bista et al. 2015). To test whether the pressure evolution during the
235 quench duration significantly controls the final run we quenched some of our 1 GPa
236 experiments under isobaric (pumped pressure at quench) conditions and conducted
237 several 1.5 GPa experiments. The maximum experimental cooling rate ranges up to 120
238 K/s (Fig. 2), which is common for piston-cylinder apparatus (e.g. Zhang et al. 2017).
239 However, the cooling rates at specific glass transition temperatures (Tg was calculated
240 after Deubener et al. 2003) are 20-90 K/s (Fig. 2), which match those for melt inclusions
241 that form in samples that range in particle size somewhere in between ash particles (>500
242 K/s) to 2 cm lapilli (up to 22 K/s; Lloyd et al. 2013; Fig. 3). Thus, the quench rates
243 achieved in the piston-cylinder closely approximate those for the most frequent size of
244 tephra samples used in melt inclusions studies. Each experiment used porous MgO parts
245 to surround the sample, and experiments were held at pressure for 5-hours at 800^{o}C in
246 order to anneal the porous MgO starting material before the temperature was increased up
247 to maximum values (1225-1300^{o}C). This annealing step prevented gold from flowing into
248 grain boundaries and pores in the MgO. Experimental durations were 16 hours for
249 1225^{o}C runs and 10 hours for 1300^{o}C runs. The run times were deemed sufficient by
250 observing homogeneous glass as a run product in low H_2O experiments. Experimental
251 conditions and run products are shown in Table 2.
252
253 **Electron microprobe analysis/characterization (EPMA)**

Always consult and cite the final, published document. See http:/www.minsocam.org or GeoscienceWorld

For each experiment, post-quenching, several 1-2 mm pieces from each experiment were prepared for analysis and characterization by electron microprobe. Experimental products were investigated for vesiculation and quench crystallization. Quantitative measurements of the major element chemistry of quenched products were obtained using the JEOL 8200 instrument installed at Washington University in St. Louis. A beam current of 25 nA, an accelerating voltage of 15 kV, and a beamsize 30 μm were used for all glass analyses. EPMA analyses of experimental run products are listed in Table 3. Chemical homogeneity of the run products was checked by multiple EPMA analyses and presented in Table 3 as standard deviation (2-sigma). Iron loss to the $Au_{80}Pd_{20}$ capsule was calculated by comparing the bulk glass composition to that of the starting material and shown to be always less than 8.5% and usually less than 1.1%.

Imaging

Images of the experimental products, presented in this study, were obtained with the following instruments: an optical microscope, the JEOL 8200 electron microprobe installed at Washington University in St. Louis as well as a JEOL JSM-6010LA analytical scanning electron microscope and a JEOL JSM-7100F field emission scanning electron microscope housed at the University of Nevada, Reno. The images are presented on Figs. 6, 9 and also in Appendices #1 and #2.

Quantitative analysis of H_2O in experimental products

To determine the dissolved H_2O of our experimental run products we used a bulk extraction technique (Ihinger et al. 1994), which is based on measuring the loss on

Always consult and cite the final, published document. See http:/www.minsocam.org or GeoscienceWorld

277 ignition of the hydrous glass. Quantification of water content was conducted using a
278 Thermogravimetric Analyzer (TGA, Q5000IR, TA Instruments) having a sensitivity of
279 0.1 μg and the weighing accuracy ± 0.1% (see method's details in Mielenz et al. 1953;
280 Knowlton et al. 1981; Guggenheim and van Groos 2001; Földvári 2011). In a typical
281 TGA analysis, 5-7 mg of sample was crushed to a fine powder in an agate mortar
282 immediately prior to the analysis. In this way we minimized H_2O loss from the sample, or
283 H_2O gain by adsorption onto the powdered sample from the atmosphere. The powdered
284 sample was placed in a platinum pan and heated at a rate of 5°C/min to 850°C under a
285 flow of N_2 (1 bar, 25 mL/min). Ultra-pure N_2 was used for all measurements. After
286 heating, the sample was held at 850°C for a time (5-30 min) until no mass change greater
287 than 1 μg per minute was observed. For each TGA run, the change in mass and
288 temperature was recorded continuously during the entire measurement. The techniques
289 that were employed in this study actually measure the total volatile content of
290 experimental run products, not just the dissolved H_2O. The major volatile component of
291 the experimental run products is H_2O, however other volatile species, primarily dissolved
292 CO_2, may contribute to the total volatile content. The run products from our experiments
293 have low amounts of CO_2 (~500 ppm; see details in the Result section). Such CO_2
294 content is small compared to the H_2O contents of these experiments, so that contribution
295 to both total volatile content and H_2O solubility during the quench are assumed to be
296 negligible (e.g. Papale et al. 2006; Métrich and Wallace 2008; Shishkina et al 2010;
297 Steele-Macinnis et al. 2011; Steele-Macinnis et al. 2017).
298 H_2O determinations by TGA analyses of our experimental products also were
299 complemented by H_2O estimations by difference from 100% totals from EPMA analysis

Always consult and cite the final, published document. See http:/www.minsocam.org or GeoscienceWorld

This is a preprint, the final version is subject to change, of the American Mineralogist (MSA)
Cite as Authors (Year) Title. American Mineralogist, in press.
DOI: https://doi.org/10.2138/am-2019-6735

("volatiles by difference" (VBD) method, e.g. Nash 1992; Devine et al. 1995; King et al. 2002; Humphreys et al. 2006; Blundy and Cashman 2008). The VBD method is widely used for quantifying the volatile contents in both of experimental (e.g. Di Carlo et al. 2006; Botcharnikov et al. 2008; Erdmann and Koepke 2016) and natural (e.g. Sommer 1977; Rutherford and Devine 1996; Métrich et al. 2004; Holtz et al. 2005) silicate glasses. The quantitative analysis of H_2O both by TGA and VBD determinations in experimental products are listed in Table 3. The estimated uncertainty for total water content using the by difference method is higher than the TGA because it takes into account the uncertainty on all the other species measured. It was shown recently that the VBD method overestimates the volatile content of hydrous glasses as much as ~1 wt% due to sub-surface charging during EPMA analysis (Hughes et al. 2019). However the two methods agree within uncertainty for all the samples measured with both methods.

Secondary ion mass spectrometry (SIMS) analysis of volatile components

Glass chips from two experimental charges (F099, n=3; F087, n=3) were mounted individually in dental resin and polished on one side. After removal from the resin using an acetone wash the chips were mounted in indium metal for SIMS (secondary ion mass spectrometer) analysis. Volatile species (H_2O, CO_2, Cl, F, and S) and P in the experimental glasses were measured on a Cameca IMS 7f-GEO ion probe at Washington University in St. Louis. The procedure was adapted from Hauri et al. (2002) measuring monovalent anions of ^{12}C, ^{16}O, ^{1}H, ^{19}F, ^{30}Si, ^{31}P, ^{32}S, and ^{35}Cl. A primary beam (5–10 nA) accelerated to 10 kV was used to create a ~20 μm spot size. We used primary basaltic reference materials ALV-519-4-1, ALV-1833-11, ALV-1846-12, ALV-1833-1

Always consult and cite the final, published document. See http:/www.minsocam.org or GeoscienceWorld

This is a preprint, the final version is subject to change, of the American Mineralogist (MSA)
Cite as Authors (Year) Title. American Mineralogist, in press.
DOI: https://doi.org/10.2138/am-2019-6735

characterized by Kumamoto et al. (2017) and Fonualei Rift:ND-60-01 (n=10) and Mangatolu Rift:ND-70-01 (n=11) as secondary reference materials (Lloyd et al. 2013). The primary reference glasses were used to develop calibration curves for H_2O, F, P, S, and Cl. Given the high background for ^{12}C for the standard mount, likely due to contamination derived from the standard mount, we used the secondary standards to obtain a calibration curve for CO_2. A significantly lower background in ^{12}C characterized the sample mount. It is noted that we report CO_2 concentrations for the experimental glasses with less confidence given that no additional secondary standard was available to confirm calculated concentrations. A synthetic pure silicate glass, Suprasil, was measured to estimate limits of detection for H_2O, F, P, and S (Table 4). CO_2 is affected in the same way as mentioned above and Cl is high in this reference glass.

Powder X-ray Diffraction

The quenched products from experiments F071, F091, and F098 were ground and then analyzed using powder X-ray diffraction (XRD) to identify mineral components. All samples were mounted in zero-background Si sample holders with a 10 mm diameter well. Measurements were made on a Bruker d8 Advance diffractometer using a Cu Kα X-ray tube and a LynxEyeXE energy-dispersive strip detector. Data were collected from 5 to 80° 2θ in 0.02° steps with 0.5 s integration time; the samples were continuously rotated at 15 revolutions per minute.

Results

Always consult and cite the final, published document. See http:/www.minsocam.org or GeoscienceWorld

Our results show that quenched mafic glasses, which retained the total pre-loaded H_2O content as dissolved H_2O, only occurred in experimental runs with less than ~9 wt% H_2O (Fig. 4), at higher pre-loaded H_2O content (up to ~21 wt%) the experiments did not quench to a homogeneous glass. Key in this analysis is both the H_2O solubility in melts and the H_2O quenchability in glasses. At the P and T conditions of our experiments, the maximum solubility of H_2O in the mafic melt should be approximately 20 wt% (Mitchell et al. 2017), far exceeding observed H_2O contents in our quench products.

Textures of the quenched experimental run products systematically changed with increasing pre-loaded H_2O contents (Fig. 5). Experiments with up to 6 wt% pre-loaded H_2O quenched to optically clear, non-vesiculated glass. For experiments with more than 6 wt% H_2O but less than 9 wt% H_2O we identify a "transition zone" where run products were not completely quenched to vesicle free glass; instead there was a mixture with areas of optically clear glass and areas of glass thoroughly permeated with quench crystals, vesicles and devitrified glass. For our experiments with >9 wt% of pre-loaded H_2O, optically clear glass was not present at any amount and all experimental products were an intimate mixture of fractured, vesicular, devitrified glass, quench crystals, and hydrous products of glass alteration (see more details about textures for every sample in the Appendix #1).

The quenched products from experiments F071 (18 wt% of H_2O), F091 (10 wt% of H_2O), and F098 (12.6 wt% of H_2O) were analyzed using powder X-ray diffraction (XRD) to identify minerals present. XRD patterns (Fig. 6) of the three run products consist of a number of broad and often asymmetric features on top of a background containing a broad feature near 30°. This background feature indicates a significant

Always consult and cite the final, published document. See http:/www.minsocam.org or GeoscienceWorld

This is a preprint, the final version is subject to change, of the American Mineralogist (MSA)
Cite as Authors (Year) Title. American Mineralogist, in press.
DOI: https://doi.org/10.2138/am-2019-6735

amorphous component, such as glass. Features in the XRD pattern at low angles (Fig. 7) are consistent with smectites (Moore and Reynolds, 1997) having a range of hydration states, with apparent d-spacings spanning ~12.5 to ~14.9 Å. The identification of smectites is further supported by the presence of asymmetric features near 19 and 34° (Fig. 6), which are (hk0) bands indicative of a turbostratically-stacked phyllosilicate. A phyllosilicate (060) feature present near 60° consists a composite peak (Fig. 7) corresponding to two or more phases with d-spacings in the range of 1.530 to 1.542 Å, indicating all phases are trioctahedral in nature (Moore and Reynolds, 1997). Additional features present in all patterns (Fig. 6) likely originate from higher-order basal reflections associated with smectites having different degrees of hydration and additional turbostratic (hk0) bands. However, some features present may also result from partial interstratification with other phyllosilicates. In addition to the above features, sample F098 contains sharp diffraction peaks near 5.9, 11.8, and 17.8° (Figs 7, 8) corresponding to the (001), (002), and (003) reflections, respectively, of chlorite. The narrow features at higher angles that are unique to this sample also likely originate from chlorite, although additional accessory crystalline phases may be present as well. While samples F098 and F071 contain two peaks from periclase, this phase is a contaminant originating from the experimental matrix outside of the reaction capsule. High-quality SEM images of those three non-glassy experimental products with comparison to a glassy one (experiment F099) are presented on Fig. 8 (more SEM images of those experiments could be found in the Appendix #2). The SEM images visually confirm the presence vast non-glassy material (Fig. 8a, 8b, 8c) having flaky appearance, which cannot be confused with the appearance of blocky, concoidally-fractured glass (Fig. 8d).

Always consult and cite the final, published document. See http:/www.minsocam.org or GeoscienceWorld

Basaltic hydrated experimental glasses F099 and F087 were analyzed by SIMS and concentrations are reported in Table 4. SIMS results agree well with how much water was initially loaded into the capsules and with other determinations of water contents after experiment. CO_2 contents determined by SIMS (note that concentrations are reported with less confidence) are 461 (F087) and 575 ppm (F099), which suggests that CO_2 did not contribute significantly to any weight loss determined by TGA. The same applies for the other volatile elements that never exceed 200 ppm.

Discussion

Solubility vs. Quenchability

The glass transition – a conversion from a liquid silicate melt to a solid glass – is an important process responsible for quenching glassy MIs, both in natural systems and experimentally. This kinetic process strongly depends on parameters such as melt polymerization degree and cooling rates (Dingwell and Webb 1990). The temperature of the glass transition (Tg) is also controlled by the amount of dissolved H_2O, which de-polymerizes a melt. While Tg of natural mafic dry melts is about 1000 K, Tg for hydrous melts are significantly lower; as low as 450 K for a melt with 20 wt% of dissolved H_2O (Deubener et al. 2003). For higher melt H_2O contents, the lower Tg requires particularly high cooling rates to quench a melt to a glass. During the quenching process the cooling rate varies (Fig. 2) and is typically highest as the quenching commences at high temperatures. Thus, melts with no or low dissolved H_2O content quench easily as the glass transition temperature is rapidly reached. In contrast, melts with a low Tg (for

Always consult and cite the final, published document. See http:/www.minsocam.org or GeoscienceWorld

This is a preprint, the final version is subject to change, of the American Mineralogist (MSA)
Cite as Authors (Year) Title. American Mineralogist, in press.
DOI: https://doi.org/10.2138/am-2019-6735

example, H_2O-rich melts) require high peak cooling rates at high temperatures, which would be sustained to low temperatures (Fig. 2).

Under normal quenching conditions for piston cylinder experiments, the quenching is achieved by shutting off power to the device. This instantaneous loss of power cools the experiment at rates (Fig. 2, 3) similar to natural erupted samples (Lloyd et al. 2013). This cooling leads to thermal contraction and a concurrent drop of pressure on the sample (Bista et al. 2015). Such pressure change may affect the run products, if the sample becomes water-oversaturated prior to reaching Tg as a consequence of pressure drop in the sample. In our experiments, we tracked the pressure change at quench in every experiment (Fig. 9). The glass transition is reached in all experiments at pressures higher than 500 MPa. Two steps were taken to test whether the pressure evolution in our experiments controls the quenchability of the sample: 1) some of our 1 GPa experiments (Table 2; Fig. 9) were quenched under isobaric (without pressure drop) conditions and 2) several 1.5 GPa experiments were conducted (see Table 2 and Fig. 9). The latter higher pressure experiments had a contraction pressure drop, but still maintained pressures over 900 MPa. All experiments, including those with the modified run procedures ended up with the same experimental results. In all cases, our observed limit of ~9 wt% dissolved H_2O in the experimental glass is much lower than the H_2O content in the melt suggested from solubility experiments that determined the H_2O solubility indirectly through partitioning into olivine (Mitchell et al. 2017). Thus, our experiments indicate that the melt to glass transition fundamentally effects how much water can remain dissolved and the release of water from the melt occurred because of the structural change related to the

Always consult and cite the final, published document. See http:/www.minsocam.org or GeoscienceWorld

This is a preprint, the final version is subject to change, of the American Mineralogist (MSA)
Cite as Authors (Year) Title. American Mineralogist, in press.
DOI: https://doi.org/10.2138/am-2019-6735

melt-glass transition and was not in response to lower H_2O solubility limits at lower pressures.

How H_2O is accommodated in the atomic structure of the glass may change during the melt-glass transition, likely due to changes in the speciation of hydrogen. In melts, water dissolves as both hydroxyl groups (OH^-) and molecular water (H_2O_m) (Stolper 1982a, 1982b; Silver and Stolper 1989; McMillan 1994). The incorporation of hydroxyl groups is well understood. Hydroxyl groups are thought to break bridging oxygen bonds and therefore easily bound structurally within the silicate melt (e.g. Mysen 2014). The structural position of molecular water in silicate melt is less clear. As a neutral, although polar species molecular water potentially behaves similarly to noble gases, which fit into holes in the melt/glass structure (Carroll and Stolper 1993; Guillot and Sarda 2006; Guillot and Sator 2012). If water occupies free volumes or structural cavities in the melt (Paonita 2005), the so-called ionic porosity (i.e., the volume of holes in the structure; Carroll and Stolper 1993) may control the solubility of water molecules in silicate melt/glass. Compared to high temperature and higher H_2O_{total} contents where water is primarily incorporated as hydroxyl groups (OH^-) into the silicate melt structure (Nowak and Behrens 1995; Chertkova and Yamashita 2015), OH^- groups convert to molecular water during cooling and quenching to a glass (Stolper 1982a, 1982b; Silver and Stolper 1989). The ratio of hydrogen bound as hydroxyl groups to molecular water (OH^-/H_2O_m) decreases from up to 4 in the melt to 0.25 in quenched glass (for an experimental charge with 8 wt% of H_2O_{total}; Chertkova and Yamashita 2015). The drastic increase in the amount of molecular H_2O during quenching may exceed the ability of the glass to accommodate water in its structural cavities. For hydrous arc magmas with 14-20

Always consult and cite the final, published document. See http:/www.minsocam.org or GeoscienceWorld

This is a preprint, the final version is subject to change, of the American Mineralogist (MSA)
Cite as Authors (Year) Title. American Mineralogist, in press.
DOI: https://doi.org/10.2138/am-2019-6735

wt% of H_2O_{total} (36-46 mol% of H_2O), quenching to glass in MIs might result in occupying all free structural cavities by molecular H_2O and exsolving excess H_2O to a fluid or gas phase (bubbles), which can promote alteration/devitrification (Anderson 1991) through crystallization of hydrous minerals and/or over pressurize the inclusion causing the host crystal to rupture.

P-T paths of experimental products at quench vs. natural MIs

When a melt inclusion forms in nature, the pressure inside and outside the olivine is equal. During magma ascent and eruption, the pressure inside the melt inclusion will be reduced due to a combination of several factors, such as elastic deformation of the host mineral, post entrapment crystallization, diffusive volatile components loss, and volume change at glass transition. The pressure inside the melt inclusion gets reduced, but does not go to zero (e.g. Steele-MacInnis et al. 2011; Gaetani et al. 2012; Hartley et al. 2014; Moore et al 2015; Wallace et al. 2015a; Steele-MacInnis et al. 2017). Some of the contributions to the pressure drop might be minimized in the case of rapid magmatic ascent, but overall partial decompression will occur. The pressure drop in a MI can be calculated (Zhang 1998) and it is about 3-4 kbar for olivine hosted MIs that are < 150 μm in size and are formed at a depth of 20-30 km (e.g. Schiano and Bourdon 1999; Maclennan 2017). This pressure drop is similar in magnitude compared to the pressure change resulting from thermal contraction during the quenching of our experiments under uncontrolled pressure conditions (described above) (Fig. 9). Moreover, even the experiments with isobaric quench produced the same run products as the experiments with a pressure drop. Thus, our experiments represent a conservative estimate for the

Always consult and cite the final, published document. See http:/www.minsocam.org or GeoscienceWorld

This is a preprint, the final version is subject to change, of the American Mineralogist (MSA)
Cite as Authors (Year) Title. American Mineralogist, in press.
DOI: https://doi.org/10.2138/am-2019-6735

maximum water content that can quench to a glass in natural melt inclusions and we suggest that decompression conditions at quench in our experiments were comparable to natural MIs.

MI re-equilibration vs. quenchability

It is often interpreted that the most water-rich melt inclusions analyzed for a given volcanic suite of samples experienced the least water loss due to diffusive re-equilibration, and thus are the best estimates we have for the highest water contents of primitive arc magmas (e.g. Métrich and Wallace 2008; Bouvet de Maisonneuve et al. 2012; Lloyd et al. 2013 and references therein). This is fundamentally different than what we are showing in this study, which is that there is a physical limit to how much water a glassy melt inclusion can hold. Because the highest values of measured dissolved H_2O in melt inclusions coincide with the experimentally determined quenching limit, it precludes the use of the melt inclusion record to determine the existence and/or prevalence of super-hydrous arc magmas. Indeed, MIs lose significant amounts of water during slow ascent of arc magma to the surface due to rapid hydrogen diffusion. But even in cases when magma ascends extremely rapidly, and keeps most of its original H_2O content, a MI with high water content (>9 wt%) is unlikely to be quenched to a glassy MI.

Deep-formed crystals are brought to the surface in arcs fairly commonly. Mantle xenoliths while not extremely abundant, are ubiquitous amongst most arcs (e.g. Bryant et al. 2007; Ionov 2010), and are much larger in size than single crystals. If xenoliths can make it to the surface from the mantle, certainly deep-formed crystals can as well. In the case of arcs there is also a common occurrences of primitive olivine and pyroxene

Always consult and cite the final, published document. See http:/www.minsocam.org or GeoscienceWorld

This is a preprint, the final version is subject to change, of the American Mineralogist (MSA)
Cite as Authors (Year) Title. American Mineralogist, in press.
DOI: https://doi.org/10.2138/am-2019-6735

phenocrysts (Mg# ≈ 90 and more; e.g. Nye and Reid 1986; Ozerov 2000; Straub et al. 2008; Ruprecht and Plank 2013; Gavrilenko et al. 2016a; 2016b; Streck and Leeman 2018), which are the very first crystals to form from melts in equilibrium with the mantle, and are most likely formed at depth. Many of those deep primitive crystals contain MIs (e.g. Churikova et al. 2007; Portnyagin et al. 2007; Johnson et al. 2008; Cooper et al. 2010; Mironov and Portnyagin 2011; Ruscitto et al. 2011; Tolstykh et al. 2012; Mironov et al. 2015; Walowski et al. (in review)) with a range in volatile contents.

What then can explain the lack of high-pressure glassy melt inclusions? There are two non-mutually exclusive mechanisms for this: re-equilibration of hydrogen at shallow pressures and the existence of super-hydrous melt inclusions that cannot quench to a glass. For melt inclusions to retain >9 wt% H_2O until eruption and quenching, they must ascend rapidly to the surface from depths where water solubility exceeds 9 wt%. Such rapid ascent has been proposed for some arc volcanoes (Gordeychik et al. 2018). We would still emphasize that H_2O re-equilibration between MIs and matrix melt is known to be fast and likely controls the final recorded H_2O content in MIs. Partial to complete re-equilibration occurs on timescales of hours to days (e.g. Qin et al. 1992; Gaetani et al. 2012; Bucholz et al. 2013) depending on the crystal and melt inclusion size, the magma temperature, and the ascent rate. However, as diffusive flux out of the melt inclusions is a direct function of the concentration gradient between the matrix melt and the melt inclusion, re-equilibration is most effective at shallow pressures, where fast ascent on the order of minutes to hours has been suggested (e.g. Demouchy et al. 2006; Humphreys et al. 2008; Lloyd et al. 2014, Ferguson et al. 2016, Zellmer et al. 2016; Petrelli et al. 2018 and references therein). In the lower crust where H_2O solubility is high the gradient of

Always consult and cite the final, published document. See http:/www.minsocam.org or GeoscienceWorld

H_2O contents between a MI and surrounding magma is small, re-equilibration is slowed. Thus, ascent driven water loss from melt inclusions below 10-12 wt% H_2O is limited until mid-crustal depth (6-7 kbar for 10-12 wt% H_2O; Shishkina et al. 2010). Rapid magma ascent is likely in some cases due to such factors as extreme buoyancy of hydrous magmas (e.g. Herzberg et al. 1983; Ochs and Lange 1999), the rapid dynamics of dike propagation (Rubin 1993; Dahm 2000; Taisne and Jaupart 2011; Rivalta et al. 2015), and absence of a crustal magma chamber for an arc volcano (Ariskin et al. 1995; Ozerov et al. 1997; Lees et al. 2007; Ozerov 2009; Mironov and Portnyagin 2011; Kayzar et al. 2014; Levin et al. 2014), which could help to preserve near-original H_2O contents in primitive melt inclusions (and avoid/minimize rapid re-equilibration of a MI with external magma).

Comparison of experimental results to natural MIs

Most mafic MIs from subduction zone settings have low H_2O content (<4 wt%; Fig. 1) presumably caused by extensive degassing and diffusive equilibration through olivine-host crystals. Emphasis in recent studies has shifted to analyzing melt inclusions from fast cooled olivine grains in tephra particles, which often show H_2O content of >4 wt%. (e.g. Johnson et al. 2008), but do not exceed 8.5 wt% of H_2O (de Moor et al. 2013). The maxima in dissolved H_2O found in quickly cooled olivine crystals (Fig 2) is normally interpreted to represent the maximum H_2O content of arc magmas (e.g. Plank et al. 2013). Our experiments provide an alternative interpretation of natural glassy MI; that this maximum content observed in nature represents a physico-chemical limit to the amount of H_2O that can be found dissolved in a glassy melt inclusion.

Always consult and cite the final, published document. See http:/www.minsocam.org or GeoscienceWorld

This is a preprint, the final version is subject to change, of the American Mineralogist (MSA)
Cite as Authors (Year) Title. American Mineralogist, in press.
DOI: https://doi.org/10.2138/am-2019-6735

Studies that focus on measuring water contents of glassy melt inclusions show that MI measurements are most abundant in the range of 1 to 6 wt% H_2O contents (99% of the data points). Finding glassy melt inclusions in this range is common and consistent with our experiments. More hydrous glassy melt inclusions become increasingly rare in what we refer to in the experiments as the "transition zone" (6-9 wt% H_2O, Fig. 1). For the experiments we propose that quenching to an optically clear single-phase glass is kinetically controlled and by analogy we expect natural MIs that form from melts with 6-9 wt% of H_2O to quench to non-glassy inclusions. Only in the rare cases where quench rates are extremely high and samples experience natural kinetic barriers to forming quench crystals (i.e. little undercooling before the glass transition is achieved) can glassy melt inclusions form. The rarity of glassy melt inclusions with high water contents is thus not directly tied to the rarity of high water content melts, but to the preferential analysis of glassy melt inclusions that get selected for study. Berndt et al. (2002) were able to quench an optically clear (bubble- and crystal-free) glass from a basaltic melt containing 9.38 wt% of H_2O using a rapid-quench device in an internally heated pressure vessel for quench rates of approximately ~150 K/s. The higher cooling rate at Tg is the likely reason why Berndt et al. (2002) obtained better quality quenched glass, than ones from our study. Indeed, this result (9.38 wt% of H_2O) is the maximum for published experiments on mafic quenched glasses, and is still consistent with our results. However, it is probably not possible to obtain such high cooling rates (~150 K/s) at Tg in natural MIs.

For our experiments with >9 wt% of loaded H_2O, optically clear glass was not present and instead an intimate mixture of fractured, vesicular, devitrified glass, quench

Always consult and cite the final, published document. See http:/www.minsocam.org or GeoscienceWorld

This is a preprint, the final version is subject to change, of the American Mineralogist (MSA)
Cite as Authors (Year) Title. American Mineralogist, in press.
DOI: https://doi.org/10.2138/am-2019-6735

crystals, and hydrous products of glass alteration comprised all experimental products. X-ray diffraction measurements on experimental run products from super-hydrous experiments show mineralogy of run products that includes low-temperature hydrous minerals (smectites, chlorite) and amorphous material that is likely poorly quenched melt. A similar mineralogy has been described in devitrified MIs in olivine (e.g. Imae and Ikeda, 2007).

There are multiple possible devitrification mechanisms, which cannot be distinguished with our current experimental setup: 1) during the quench, water exsolves and alters the glass in the experiment producing a palagonite-like substance (Bonatti 1965), which is basically a mixture of a variety of smectites and potentially zeolites and oxides (Stroncik and Schmincke 2002); 2) a devitrification mechanism where the crystallization temperature of hydrous minerals is higher than the Tg and this leads to the nucleation and crystallization of hydrous minerals before a glass transition. A more detailed documentation of the devitrification mechanism would require in situ observations. Nevertheless, natural melt inclusions with H_2O contents above 9 wt% most likely never quench to a glass, and form devitrified inclusions (Anderson 1991; Imae and Ikeda, 2007) or exsolve water that may over pressurize the inclusion and break the host crystal (decrepitation, e.g. Wanamaker et al. 1990).

Our results indicate that 9 wt% of dissolved H_2O is a physical limit for silicate mafic melts to quench to a homogeneous glass under naturally-occurring cooling rates (Fig. 4). Thus, the observed maximum of 8-9 wt% H_2O from glassy mafic MI studies may correspond to a quenchability limit (Fig. 1). We speculate that melt inclusions of H_2O-rich magmas (>9 wt% H_2O) may exist, but they may never get preserved as glassy

Always consult and cite the final, published document. See http:/www.minsocam.org or GeoscienceWorld

This is a preprint, the final version is subject to change, of the American Mineralogist (MSA)
Cite as Authors (Year) Title. American Mineralogist, in press.
DOI: https://doi.org/10.2138/am-2019-6735

MIs. Therefore, studies that focus solely on glassy single-phase MIs in olivine (or any mineral host) will systematically be limited to finding dissolved water contents less than 8-9 wt% and therefore may not fully characterize the magmatic H_2O budget in subduction zones.

Implications

Our hydrothermal experiments show that the maxima of 8-9 wt% of dissolved H_2O from MIs studies matches the physicochemical limit of quenched glassy-melt inclusions. At higher dissolved H_2O contents and natural quenching rates mafic melts cannot form glassy MIs. The possibility that such a limit for glassy MIs exists has never before been directly studied experimentally and requires a reevaluation of using MIs as a primary tool to estimate global water fluxes at arcs. MIs likely form at all depths where crystallization occurs, and the lack of deep formed and equilibrated MIs in the existing literature suggests there might be a higher probability for super-hydrous (>9 wt% of H_2O) magmas than previously recognized. The results of this study have identified five main closing thoughts:

- Glassy MIs are excellent recorders of pre-eruptive H_2O contents in the upper-most part of the crust, where the solubility limit for hydrous magmas is less than 6-7 wt% H_2O. Thus, MI studies focusing on degassing and eruption-style phenomena are not affected by our results.
- A higher abundance of magmas containing >10 wt% of H_2O may explain why dense primitive magmas in convergent margins can quickly reach the surface without much crystallization and fractionation (Herzberg et al. 1983; Kohn et al.

Always consult and cite the final, published document. See http:/www.minsocam.org or GeoscienceWorld

This is a preprint, the final version is subject to change, of the American Mineralogist (MSA)
Cite as Authors (Year) Title. American Mineralogist, in press.
DOI: https://doi.org/10.2138/am-2019-6735

1989; Ruprecht and Plank 2013), despite a low-density filter in the form of evolved magmas and crust in their path.

- Because glass quenchability is dependent on the amount of water in a mafic sample, MI studies that focus on single-phase glassy MIs are introducing a previously unrecognized sampling bias into our understanding of primitive magmas.
- Our findings suggest that examining the mineralogy of non-glassy melt inclusions found in quickly cooled environments such as small lapilli or even ash deposits for the presence of chlorites or smectites may be used to identify super-hydrous magmas.
- Estimates of total water contents returned to the crust/atmosphere by tectonic recycling based on studies of MIs (e.g. Straub and Layne 2003; Wallace 2005; Parai and Mukhopadhyay 2012; Wallace et al. 2015b; Peslier et al. 2017) likely underestimate the amount of returned H_2O. Recent geophysical studies (Cai et al 2018) also see evidence for more extensive hydration of incoming slabs at arcs, which support the idea more H_2O is getting returned to the surface through subduction zones than previously recognized.

Acknowledgments

We thank Paul Carpenter for invaluable assistance with EPMA analyses at Washington University in St. Louis. Additionally we are grateful to Tatiana Shishkina for thorough discussion and to Hélène Couvy for her comprehensive assistance in lab work. Maxim Portnyagin, Glenn Gaetani, Adam Kent, Thomas Sisson, and Michel Pichavant are

Always consult and cite the final, published document. See http:/www.minsocam.org or GeoscienceWorld

This is a preprint, the final version is subject to change, of the American Mineralogist (MSA)
Cite as Authors (Year) Title. American Mineralogist, in press.
DOI: https://doi.org/10.2138/am-2019-6735

sincerely thanked for providing insightful comments and criticism, which helped us to rethink some of our ideas and sharpened the discussion of the paper. Constructive reviews from Matthew Steele-MacInnis, Michael Rowe and one anonymous reviewer improved the clarity of our arguments and data presentation. We would like to thank Kyle Ashley for his editorial handling of the manuscript. MG acknowledges support from McDonnell Center for the Space Sciences. MK acknowledges support from US National Science Foundation grant EAR 1654683. PR acknowledges support from US National Science Foundation grant EAR 1719687. JGC acknowledges support from US National Aeronautics and Space Administration grant NNX14AJ95G.

References cited

Anderson, A.T. (1991) Hourglass inclusions: Theory and application to the Bishop Rhyolitic Tuff. American Mineralogist, 76(1-2), 530-547.

Ariskin, A.A., Barmina, G.S., Ozerov, A.Y., and Nielsen, R.L. (1995) Genesis of high-alumina basalts from Klyuchevskoi volcano. Petrology, 3(5), 449-472.

Auer, S., Bindeman, I., Wallace, P., Ponomareva, V., and Portnyagin, M. (2009) The origin of hydrous, high-$\delta^{18}O$ voluminous volcanism: diverse oxygen isotope values and high magmatic water contents within the volcanic record of Klyuchevskoy volcano, Kamchatka, Russia. Contributions to Mineralogy and Petrology, 157(2), 209-230, doi:10.1007/s00410-008-0330-0.

Ayers, J.C., Brenan, J.B., Watson, E.B., Wark, D.A., and Minarik, W.G. (1992) A new capsule technique for hydrothermal experiments using the piston-cylinder apparatus. American Mineralogist, 77(9-10), 1080-1086.

Always consult and cite the final, published document. See http:/www.minsocam.org or GeoscienceWorld

665 Baker, D.R., and Alletti, M. (2012) Fluid saturation and volatile partitioning between
666 melts and hydrous fluids in crustal magmatic systems: The contribution of
667 experimental measurements and solubility models. Earth-Science Reviews,
668 114(3–4), 298-324, doi:10.1016/j.earscirev.2012.06.005.
669 Baker, M.B., Grove, T.L., and Price, R. (1994) Primitive basalts and andesites from the
670 Mt. Shasta region, N. California: products of varying melt fraction and water
671 content. Contributions to Mineralogy and Petrology, 118(2), 111-129,
672 doi:10.1007/bf01052863.
673 Behrens, H., Misiti, V., Freda, C., Vetere, F., Botcharnikov, R.E., and Scarlato, P. (2009)
674 Solubility of H_2O and CO_2 in ultrapotassic melts at 1200 and 1250°C and pressure
675 from 50 to 500 MPa. American Mineralogist, 94(1), 105-120,
676 doi:10.2138/am.2009.2796.
677 Berndt, J., Liebske, C., Holtz, F., Freise, M., Nowak, M., Ziegenbein, D., Hurkuck, W.,
678 and Koepke, J. (2002) A combined rapid-quench and H_2-membrane setup for
679 internally heated pressure vessels: Description and application for water solubility
680 in basaltic melts. American Mineralogist, 87(11-12), 1717-1726, doi:10.2138/am-
681 2002-11-1222.
682 Bista, S., Stebbins, J.F., Hankins, W.B., and Sisson, T.W. (2015) Aluminosilicate melts
683 and glasses at 1 to 3 GPa: Temperature and pressure effects on recovered
684 structural and density changes. American Mineralogist, 100(10), 2298-2307,
685 doi:10.2138/am-2015-5258.
686 Blundy, J., and Cashman, K. (2008) Petrologic Reconstruction of Magmatic System
687 Variables and Processes. Reviews in Mineralogy and Geochemistry, 69(1), 179-

Always consult and cite the final, published document. See http:/www.minsocam.org or GeoscienceWorld

This is a preprint, the final version is subject to change, of the American Mineralogist (MSA)
Cite as Authors (Year) Title. American Mineralogist, in press.
DOI: https://doi.org/10.2138/am-2019-6735

239, doi:10.2138/rmg.2008.69.6.

Bonatti, E. (1965) Palagonite, hyaloclastites and alteration of volcanic glass in the ocean. Bulletin Volcanologique, 28(1), 257-269, doi:10.1007/bf02596930.

Botcharnikov, R.E., Almeev, R.R., Koepke, J., and Holtz, F. (2008) Phase Relations and Liquid Lines of Descent in Hydrous Ferrobasalt—Implications for the Skaergaard Intrusion and Columbia River Flood Basalts. Journal of Petrology, 49(9), 1687-1727, doi:10.1093/petrology/egn043.

Bouvet de Maisonneuve, C., Dungan, M.A., Bachmann, O., and Burgisser, A. (2012) Insights into shallow magma storage and crystallization at Volcán Llaima (Andean Southern Volcanic Zone, Chile). Journal of Volcanology and Geothermal Research, 211-212, 76-91, doi:10.1016/j.jvolgeores.2011.09.010.

Boyd, F.R., and England, J.L. (1960) Apparatus for phase-equilibrium measurements at pressures up to 50 kilobars and temperatures up to 1750°C. Journal of Geophysical Research, 65(2), 741-748, doi:10.1029/JZ065i002p00741.

Brenan, J.M., Shaw, H.F., Phinney, D.L., and Ryerson, F.J. (1994) Rutile-aqueous fluid partitioning of Nb, Ta, Hf, Zr, U and Th: implications for high field strength element depletions in island-arc basalts. Earth and Planetary Science Letters, 128(3), 327-339, doi:10.1016/0012-821X(94)90154-6.

Brenan, J.M., Shaw, H.F., Ryerson, F.J., and Phinney, D.L. (1995) Mineral-aqueous fluid partitioning of trace elements at 900°C and 2.0 GPa: Constraints on the trace element chemistry of mantle and deep crustal fluids. Geochimica et Cosmochimica Acta, 59(16), 3331-3350, doi:10.1016/0016-7037(95)00215-L.

Bryant, J.A., Yogodzinski, G.M., and Churikova, T.G. (2007) Melt-mantle interactions

Always consult and cite the final, published document. See http:/www.minsocam.org or GeoscienceWorld

This is a preprint, the final version is subject to change, of the American Mineralogist (MSA)
Cite as Authors (Year) Title. American Mineralogist, in press.
DOI: https://doi.org/10.2138/am-2019-6735

711 beneath the Kamchatka arc: Evidence from ultramafic xenoliths from Shiveluch
712 volcano. Geochemistry Geophysics Geosystems, 8 (4), Q04007,
713 doi:10.1029/2006gc001443.
714 Bucholz, C.E., Gaetani, G.A., Behn, M.D., and Shimizu, N. (2013) Post-entrapment
715 modification of volatiles and oxygen fugacity in olivine-hosted melt inclusions.
716 Earth and Planetary Science Letters, 374, 145-155,
717 doi:10.1016/j.epsl.2013.05.033.
718 Cai, C., Wiens, D.A., Shen, W., and Eimer, M. (2018) Water input into the Mariana
719 subduction zone estimated from ocean-bottom seismic data. Nature, 563(7731),
720 389-392, doi:10.1038/s41586-018-0655-4.
721 Carmichael, I.S. (2002) The andesite aqueduct: perspectives on the evolution of
722 intermediate magmatism in west-central (105–99°W) Mexico. Contributions to
723 Mineralogy and Petrology, 143(6), 641-663, doi:10.1007/s00410-002-0370-9.
724 Carroll, M.R., and Stolper, E.M. (1993) Noble gas solubilities in silicate melts and
725 glasses: New experimental results for argon and the relationship between
726 solubility and ionic porosity. Geochimica et Cosmochimica Acta, 57(23), 5039-
727 5051, doi:10.1016/0016-7037(93)90606-W.
728 Cashman, K.V. (2004) Volatile Controls on Magma Ascent and Eruption. The State of
729 the Planet: Frontiers and Challenges in Geophysics, 150, p. 109-124. American
730 Geophysical Union.
731 Chen, Y., Provost, A., Schiano, P., and Cluzel, N. (2011) The rate of water loss from
732 olivine-hosted melt inclusions. Contributions to Mineralogy and Petrology,
733 162(3), 625-636, doi:10.1007/s00410-011-0616-5.

Always consult and cite the final, published document. See http:/www.minsocam.org or GeoscienceWorld

This is a preprint, the final version is subject to change, of the American Mineralogist (MSA)
Cite as Authors (Year) Title. American Mineralogist, in press.
DOI: https://doi.org/10.2138/am-2019-6735

734 Chertkova, N., and Yamashita, S. (2015) In situ spectroscopic study of water speciation
735 in the depolymerized $Na_2Si_2O_5$ melt. Chemical Geology, 409, 149-156,
736 doi:10.1016/j.chemgeo.2015.05.012.
737 Churikova, T., Wörner, G., Mironov, N., and Kronz, A. (2007) Volatile (S, Cl and F) and
738 fluid mobile trace element compositions in melt inclusions: implications for
739 variable fluid sources across the Kamchatka arc. Contributions to Mineralogy and
740 Petrology, 154(2), 217-239, doi:10.1007/s00410-007-0190-z.
741 Cooper, L.B., Plank, T., Arculus, R.J., Hauri, E.H., Hall, P.S., and Parman, S.W. (2010)
742 High-Ca boninites from the active Tonga Arc. Journal of Geophysical Research:
743 Solid Earth, 115(B10), B10206, doi:10.1029/2009JB006367.
744 Cottrell, E., and Kelley, K.A. (2011) The oxidation state of Fe in MORB glasses and the
745 oxygen fugacity of the upper mantle. Earth and Planetary Science Letters, 305(3–
746 4), 270-282, doi:10.1016/j.epsl.2011.03.014.
747 Dahm, T. (2000) On the shape and velocity of fluid-filled fractures in the Earth.
748 Geophysical Journal International, 142(1), 181-192, doi:10.1046/j.1365-
749 246x.2000.00148.x.
750 Danyushevsky, L.V., McNeill, A.W., and Sobolev, A.V. (2002) Experimental and
751 petrological studies of melt inclusions in phenocrysts from mantle-derived
752 magmas: an overview of techniques, advantages and complications. Chemical
753 Geology, 183(1–4), 5-24, doi:10.1016/S0009-2541(01)00369-2.
754 de Moor, J.M., Fischer, T.P., King, P.L., Botcharnikov, R.E., Hervig, R.L., Hilton, D.R.,
755 Barry, P.H., Mangasini, F., and Ramirez, C. (2013) Volatile-rich silicate melts
756 from Oldoinyo Lengai volcano (Tanzania): Implications for carbonatite genesis

Always consult and cite the final, published document. See http:/www.minsocam.org or GeoscienceWorld

This is a preprint, the final version is subject to change, of the American Mineralogist (MSA)
Cite as Authors (Year) Title. American Mineralogist, in press.
DOI: https://doi.org/10.2138/am-2019-6735

and eruptive behavior. Earth and Planetary Science Letters, 361, 379-390, doi:10.1016/j.epsl.2012.11.006.

Demouchy, S., Jacobsen, S.D., Gaillard, F., and Stern, C.R. (2006) Rapid magma ascent recorded by water diffusion profiles in mantle olivine. Geology, 34(6), 429-432, doi:10.1130/g22386.1.

Deubener, J., Müller, R., Behrens, H., and Heide, G. (2003) Water and the glass transition temperature of silicate melts. Journal of Non-Crystalline Solids, 330(1), 268-273, doi:10.1016/S0022-3093(03)00472-1.

Devine, J.D., Gardner, J.E., Brack, H.P., Layne, G.D., and Rutherford, M.J. (1995) Comparison of microanalytical methods for estimating H_2O contents of silicic volcanic glasses. American Mineralogist, 80(3-4), 319-328, doi:10.2138/am-1995-3-413.

Di Carlo, I.D.A., Pichavant, M., Rotolo, S.G., and Scaillet, B. (2006) Experimental Crystallization of a High-K Arc Basalt: the Golden Pumice, Stromboli Volcano (Italy). Journal of Petrology, 47(7), 1317-1343, doi:10.1093/petrology/egl011.

Di Genova, D., Vasseur, J., Hess, K.-U., Neuville, D.R., and Dingwell, D.B. (2017) Effect of oxygen fugacity on the glass transition, viscosity and structure of silica- and iron-rich magmatic melts. Journal of Non-Crystalline Solids, 470, 78-85, doi:10.1016/j.jnoncrysol.2017.05.013.

Dingwell, D.B., and Webb, S.L. (1990) Relaxation in silicate melts. European Journal of Mineralogy, 2(4), 427-449, doi:10.1127/ejm/2/4/0427.

Erdmann, M., and Koepke, J. (2016) Silica-rich lavas in the oceanic crust: experimental evidence for fractional crystallization under low water activity. Contributions to

Always consult and cite the final, published document. See http:/www.minsocam.org or GeoscienceWorld

This is a preprint, the final version is subject to change, of the American Mineralogist (MSA)
Cite as Authors (Year) Title. American Mineralogist, in press.
DOI: https://doi.org/10.2138/am-2019-6735

780 Mineralogy and Petrology, 171(10), 83, doi:10.1007/s00410-016-1294-0.
781 Esposito, R., Lamadrid, H.M., Redi, D., Steele-MacInnis, M., Bodnar, R.J., Manning,
782 C.E., De Vivo, B., Cannatelli, C., and Lima, A. (2016) Detection of liquid H_2O in
783 vapor bubbles in reheated melt inclusions: Implications for magmatic fluid
784 composition and volatile budgets of magmas? American Mineralogist, 101(7),
785 1691-1695, doi:10.2138/am-2016-5689.
786 Ferguson, D.J., Gonnermann, H.M., Ruprecht, P., Plank, T., Hauri, E.H., Houghton, B.F.,
787 and Swanson, D.A. (2016) Magma decompression rates during explosive
788 eruptions of Kīlauea volcano, Hawaii, recorded by melt embayments. Bulletin of
789 Volcanology, 78(10), 1-12, doi:10.1007/s00445-016-1064-x.
790 Fischer, T.P., and Marty, B. (2005) Volatile abundances in the sub-arc mantle: insights
791 from volcanic and hydrothermal gas discharges. Journal of Volcanology and
792 Geothermal Research, 140(1–3), 205-216, doi:10.1016/j.jvolgeores.2004.07.022.
793 Földvári, M. (2011) Handbook of Thermogravimetric System of Minerals and Its Use in
794 Geological Practice. 179 p. Geological Institute of Hungary (=Magyar Állami
795 Földtani Intézet).
796 Frezzotti, M.-L. (2001) Silicate-melt inclusions in magmatic rocks: applications to
797 petrology. Lithos, 55(1), 273-299, doi:10.1016/S0024-4937(00)00048-7
798 Gaetani, G.A., O'Leary, J.A., Shimizu, N., Bucholz, C.E., and Newville, M. (2012)
799 Rapid reequilibration of H_2O and oxygen fugacity in olivine-hosted melt
800 inclusions. Geology, 40(10), 915-918, doi:10.1130/g32992.1.
801 Gaetani, G.A., and Watson, E.B. (2000) Open system behavior of olivine-hosted melt
802 inclusions. Earth and Planetary Science Letters, 183(1–2), 27-41,

Always consult and cite the final, published document. See http:/www.minsocam.org or GeoscienceWorld

This is a preprint, the final version is subject to change, of the American Mineralogist (MSA)
Cite as Authors (Year) Title. American Mineralogist, in press.
DOI: https://doi.org/10.2138/am-2019-6735

doi:10.1016/S0012-821X(00)00260-0.

Gavrilenko, M., Herzberg, C., Vidito, C., Carr, M.J., Tenner, T., and Ozerov, A. (2016a) A Calcium-in-Olivine Geohygrometer and its Application to Subduction Zone Magmatism. Journal of Petrology, 57(9), 1811-1832, doi:10.1093/petrology/egw062.

Gavrilenko, M., Ozerov, A., Kyle, P.R., Carr, M.J., Nikulin, A., Vidito, C., and Danyushevsky, L. (2016b) Abrupt transition from fractional crystallization to magma mixing at Gorely volcano (Kamchatka) after caldera collapse. Bulletin of Volcanology, 78:47, doi:10.1007/s00445-016-1038-z.

GEOROC, 2018. Geochemistry of rocks of the Oceans and Continents. MPI für Chemie, Mainz, Germany. http://georoc.mpch-mainz.gwdg.de/georoc/.

Gordeychik, B., Churikova, T., Kronz, A., Sundermeyer, C., Simakin, A., and Wörner, G. (2018) Growth of, and diffusion in, olivine in ultra-fast ascending basalt magmas from Shiveluch volcano. Scientific Reports, 8(1), 11775, doi:10.1038/s41598-018-30133-1.

Grove, T., Elkins-Tanton, L., Parman, S., Chatterjee, N., Müntener, O., and Gaetani, G. (2003) Fractional crystallization and mantle-melting controls on calc-alkaline differentiation trends. Contributions to Mineralogy and Petrology, 145(5), 515-533, doi:10.1007/s00410-003-0448-z.

Grove, T.L., Baker, M.B., Price, R.C., Parman, S.W., Elkins-Tanton, L.T., Chatterjee, N., and Müntener, O. (2005) Magnesian andesite and dacite lavas from Mt. Shasta, northern California: products of fractional crystallization of H_2O-rich mantle melts. Contributions to Mineralogy and Petrology, 148(5), 542-565,

Always consult and cite the final, published document. See http:/www.minsocam.org or GeoscienceWorld

This is a preprint, the final version is subject to change, of the American Mineralogist (MSA)
Cite as Authors (Year) Title. American Mineralogist, in press.
DOI: https://doi.org/10.2138/am-2019-6735

826 doi:10.1007/s00410-004-0619-6.
827 Grove, T.L., Chatterjee, N., Parman, S.W., and Médard, E. (2006) The influence of H_2O
828 on mantle wedge melting. Earth and Planetary Science Letters, 249(1–2), 74-89,
829 doi:10.1016/j.epsl.2006.06.043.
830 Grove, T.L., Till, C.B., and Krawczynski, M.J. (2012) The Role of H_2O in Subduction
831 Zone Magmatism. Annual Review of Earth and Planetary Sciences, 40(1), 413-
832 439, doi:10.1146/annurev-earth-042711-105310.
833 Guggenheim, S., and van Groos, A.F.K. (2001) Baseline Studies of the Clay Minerals
834 Society Source Clays: Thermal Analysis. Clays and Clay Minerals, 49(5), 433-
835 443, doi:10.1346/CCMN.2001.0490509.
836 Guillot, B., and Sarda, P. (2006) The effect of compression on noble gas solubility in
837 silicate melts and consequences for degassing at mid-ocean ridges. Geochimica et
838 Cosmochimica Acta, 70(5), 1215-1230, doi:10.1016/j.gca.2005.11.007.
839 Guillot, B., and Sator, N. (2012) Noble gases in high-pressure silicate liquids: A
840 computer simulation study. Geochimica et Cosmochimica Acta, 80, 51-69,
841 doi:10.1016/j.gca.2011.11.040.
842 Hacker, B.R. (2008) H_2O subduction beyond arcs. Geochemistry, Geophysics,
843 Geosystems, 9(3), Q03001, doi:10.1029/2007GC001707.
844 Hacker, B.R., Abers, G.A., and Peacock, S.M. (2003) Subduction factory 1. Theoretical
845 mineralogy, densities, seismic wave speeds, and H_2O contents. Journal of
846 Geophysical Research: Solid Earth, 108(B1), doi:10.1029/2001JB001127.
847 Hamilton, D.L., Burnham, C.W., and Osborn, E.F. (1964) The Solubility of Water and
848 Effects of Oxygen Fugacity and Water Content on Crystallization in Mafic

Always consult and cite the final, published document. See http:/www.minsocam.org or GeoscienceWorld

849 Magmas. Journal of Petrology, 5(1), 21-39, doi:10.1093/petrology/5.1.21.
850 Hartley, M.E., Maclennan, J., Edmonds, M., and Thordarson, T. (2014) Reconstructing
851 the deep CO_2 degassing behaviour of large basaltic fissure eruptions. Earth and
852 Planetary Science Letters, 393, 120-131, doi:10.1016/j.epsl.2014.02.031.
853 Hartley, M.E., Neave, D.A., Maclennan, J., Edmonds, M., and Thordarson, T. (2015)
854 Diffusive over-hydration of olivine-hosted melt inclusions. Earth and Planetary
855 Science Letters, 425, 168-178, doi:10.1016/j.epsl.2015.06.008.
856 Hauri, E. (2002) SIMS analysis of volatiles in silicate glasses, 2: isotopes and abundances
857 in Hawaiian melt inclusions. Chemical Geology, 183(1–4), 115-141,
858 doi:10.1016/S0009-2541(01)00374-6.
859 Hauri, E., Wang, J., Dixon, J.E., King, P.L., Mandeville, C., and Newman, S. (2002)
860 SIMS analysis of volatiles in silicate glasses: 1. Calibration, matrix effects and
861 comparisons with FTIR. Chemical Geology, 183(1), 99-114, doi:10.1016/S0009-
862 2541(01)00375-8.
863 Herzberg, C.T., Fyfe, W.S., and Carr, M.J. (1983) Density constraints on the formation of
864 the continental Moho and crust. Contributions to Mineralogy and Petrology,
865 84(1), 1-5, doi:10.1007/bf01132324.
866 Holtz, F., Sato, H., Lewis, J., Behrens, H., and Nakada, S. (2005) Experimental Petrology
867 of the 1991–1995 Unzen Dacite, Japan. Part I: Phase Relations, Phase
868 Composition and Pre-eruptive Conditions. Journal of Petrology, 46(2), 319-337,
869 doi:10.1093/petrology/egh077.
870 Hughes, E.C., Buse, B., Kearns, S.L., Blundy, J.D., Kilgour, G., and Mader, H.M. (2019)
871 Low analytical totals in EPMA of hydrous silicate glass due to sub-surface

Always consult and cite the final, published document. See http:/www.minsocam.org or GeoscienceWorld

872 charging: Obtaining accurate volatiles by difference. Chemical Geology, 505, 48-
873 56, doi:10.1016/j.chemgeo.2018.11.015.
874 Humphreys, M.C.S., Kearns, S.L., and Blundy, J.D. (2006) SIMS investigation of
875 electron-beam damage to hydrous, rhyolitic glasses: Implications for melt
876 inclusion analysis. American Mineralogist, 91(4), 667-679,
877 doi:10.2138/am.2006.1936.
878 Humphreys, M.C.S., Menand, T., Blundy, J.D., and Klimm, K. (2008) Magma ascent
879 rates in explosive eruptions: Constraints from H_2O diffusion in melt inclusions.
880 Earth and Planetary Science Letters, 270(1), 25-40,
881 doi:10.1016/j.epsl.2008.02.041.
882 Ihinger, P.D., Hervig, R.L., and McMillan, P.F. (1994) Analytical methods for volatiles
883 in glasses. Reviews in Mineralogy and Geochemistry, 30(1), 67-121.
884 Imae, N., and Ikeda, Y. (2007) Petrology of the Miller Range 03346 nakhlite in
885 comparison with the Yamato-000593 nakhlite. Meteoritics & Planetary Science,
886 42(2), 171-184, doi:10.1111/j.1945-5100.2007.tb00225.x.
887 Ionov, D.A. (2010) Petrology of Mantle Wedge Lithosphere: New Data on Supra-
888 Subduction Zone Peridotite Xenoliths from the Andesitic Avacha Volcano,
889 Kamchatka. Journal of Petrology, 51(1-2), 327-361,
890 doi:10.1093/petrology/egp090.
891 Johnson, E.R., Wallace, P.J., Cashman, K.V., Granados, H.D., and Kent, A.J.R. (2008)
892 Magmatic volatile contents and degassing-induced crystallization at Volcán
893 Jorullo, Mexico: Implications for melt evolution and the plumbing systems of
894 monogenetic volcanoes. Earth and Planetary Science Letters, 269(3–4), 478-487,

Always consult and cite the final, published document. See http:/www.minsocam.org or GeoscienceWorld

This is a preprint, the final version is subject to change, of the American Mineralogist (MSA)
Cite as Authors (Year) Title. American Mineralogist, in press.
DOI: https://doi.org/10.2138/am-2019-6735

doi:10.1016/j.epsl.2008.03.004.

Katz, R.F., Spiegelman, M., and Langmuir, C.H. (2003) A new parameterization of hydrous mantle melting. Geochemistry, Geophysics, Geosystems, 4(9), 1073, doi:10.1029/2002GC000433.

Kayzar, T.M., Nelson, B.K., Bachmann, O., Bauer, A.M., and Izbekov, P.E. (2014) Deciphering petrogenic processes using Pb isotope ratios from time-series samples at Bezymianny and Klyuchevskoy volcanoes, Central Kamchatka Depression. Contributions to Mineralogy and Petrology, 168: 1067, doi:10.1007/s00410-014-1067-6.

Kent, A.J.R. (2008) Melt Inclusions in Basaltic and Related Volcanic Rocks. Reviews in Mineralogy and Geochemistry, 69(1), 273-331, doi:10.2138/rmg.2008.69.8.

King, P.L., Vennemann, T.W., Holloway, J.R., Hervig, R.L., Lowenstern, J.B., and Forneris, J.F. (2002) Analytical techniques for volatiles: A case study using intermediate (andesitic) glasses. American Mineralogist, 87(8-9), 1077-1089, doi:10.2138/am-2002-8-904.

Knowlton, G.D., White, T.R., and McKague, H.L. (1981) Thermal study of types of water associated with clinoptilolite. Clays & Clay Minerals, 29(5), 403-411, doi:10.1346/CCMN.1981.0290510.

Kohn, S.C., Henderson, C.M.B., and Mason, R.A. (1989) Element zoning trends in olivine phenocrysts from a supposed primary high-magnesian andesite: an electron- and ion-microprobe study. Contributions to Mineralogy and Petrology, 103(2), 242-252, doi:10.1007/bf00378510.

Krawczynski, M.J., Grove, T.L., and Behrens, H. (2012) Amphibole stability in primitive

Always consult and cite the final, published document. See http:/www.minsocam.org or GeoscienceWorld

arc magmas: effects of temperature, H_2O content, and oxygen fugacity. Contributions to Mineralogy and Petrology, 164(2), 317-339, doi:10.1007/s00410-012-0740-x.

Kumamoto, K.M., Warren, J.M., and Hauri, E.H. (2017) New SIMS reference materials for measuring water in upper mantle minerals. American Mineralogist, 102(3), 537-547, doi:10.2138/am-2017-5863CCBYNCND.

Lees, J.M., Symons, N., Chubarova, O., Gorelchik, V., and Ozerov, A. (2007) Tomographic Images of Klyuchevskoy Volcano P-Wave Velocity. Volcanism and Subduction: The Kamchatka Region, p. 293-302. American Geophysical Union.

Levin, V., Droznina, S., Gavrilenko, M., Carr, M.J., and Senyukov, S. (2014) Seismically active subcrustal magma source of the Klyuchevskoy volcano in Kamchatka, Russia. Geology, 42(11), 983-986, doi:10.1130/g35972.1.

Lloyd, A., Plank, T., Ruprecht, P., Hauri, E., and Rose, W. (2013) Volatile loss from melt inclusions in pyroclasts of differing sizes. Contributions to Mineralogy and Petrology, 165(1), 129-153, doi:10.1007/s00410-012-0800-2.

Lloyd, A.S., Ruprecht, P., Hauri, E.H., Rose, W., Gonnermann, H.M., and Plank, T. (2014) NanoSIMS results from olivine-hosted melt embayments: Magma ascent rate during explosive basaltic eruptions. Journal of Volcanology and Geothermal Research, 283, 1-18, doi:10.1016/j.jvolgeores.2014.06.002.

Maclennan, J. (2017) Bubble formation and decrepitation control the CO_2 content of olivine-hosted melt inclusions. Geochemistry, Geophysics, Geosystems, 18(2), 597-616, doi:10.1002/2016GC006633.

Massare, D., Métrich, N., and Clocchiatti, R. (2002) High-temperature experiments on

Always consult and cite the final, published document. See http:/www.minsocam.org or GeoscienceWorld

941 silicate melt inclusions in olivine at 1 atm: inference on temperatures of
942 homogenization and H_2O concentrations. Chemical Geology, 183(1–4), 87-98,
943 doi:10.1016/S0009-2541(01)00373-4.
944 McGary, R.S., Evans, R.L., Wannamaker, P.E., Elsenbeck, J., and Rondenay, S. (2014)
945 Pathway from subducting slab to surface for melt and fluids beneath Mount
946 Rainier. Nature, 511(7509), 338-340, doi:10.1038/nature13493.
947 McMillan, P.F. (1994) Water solubility and speciation models. Reviews in Mineralogy
948 and Geochemistry, 30(1), 132-156.
949 Métrich, N., Allard, P., Spilliaert, N., Andronico, D., and Burton, M. (2004) 2001 flank
950 eruption of the alkali- and volatile-rich primitive basalt responsible for Mount
951 Etna's evolution in the last three decades. Earth and Planetary Science Letters,
952 228(1), 1-17, doi:10.1016/j.epsl.2004.09.036.
953 Métrich, N., and Wallace, P.J. (2008) Volatile Abundances in Basaltic Magmas and Their
954 Degassing Paths Tracked by Melt Inclusions. Reviews in Mineralogy and
955 Geochemistry, 69(1), 363-402, doi:10.2138/rmg.2008.69.10.
956 Mielenz, R.C., Schieltz, N.C., and King, M.E. (1953) Thermogravimetric analysis of clay
957 and clay-like minerals. Clays and Clay Minerals(2), 285-314,
958 doi:10.1346/CCMN.1953.0020124.
959 Mironov, N., Portnyagin, M., Botcharnikov, R., Gurenko, A., Hoernle, K., and Holtz, F.
960 (2015) Quantification of the CO_2 budget and H_2O–CO_2 systematics in subduction-
961 zone magmas through the experimental hydration of melt inclusions in olivine at
962 high H_2O pressure. Earth and Planetary Science Letters, 425, 1-11,
963 doi:10.1016/j.epsl.2015.05.043.

Always consult and cite the final, published document. See http:/www.minsocam.org or GeoscienceWorld

(Revision 2)

964 Mironov, N.L., and Portnyagin, M.V. (2011) H_2O and CO_2 in parental magmas of
965 Kliuchevskoi volcano inferred from study of melt and fluid inclusions in olivine.
966 Russian Geology and Geophysics, 52(11), 1353-1367,
967 doi:10.1016/j.rgg.2011.10.007.
968 Mitchell, A.L., Gaetani, G.A., O'Leary, J.A., and Hauri, E.H. (2017) H_2O solubility in
969 basalt at upper mantle conditions. Contributions to Mineralogy and Petrology,
970 172(10), 85, doi:10.1007/s00410-017-1401-x.
971 Moore, D., and Reynolds Jr, R. (1997) X-Ray Diffraction and the Identification and
972 Analysis of Clay Minerals. 378 p. Oxford University Press, Oxford, New York.
973 Moore, G. (2008) Interpreting H_2O and CO_2 Contents in Melt Inclusions: Constraints
974 from Solubility Experiments and Modeling. Reviews in Mineralogy and
975 Geochemistry, 69(1), 333-362, doi:10.2138/rmg.2008.69.9.
976 Moore, G., Vennemann, T., and Carmichael, I.S.E. (1998) An empirical model for the
977 solubility of H_2O in magmas to 3 kilobars. American Mineralogist, 83(1-2), 36-
978 42, doi:10.2138/am-1998-1-203.
979 Moore, L.R., Gazel, E., Tuohy, R., Lloyd, A.S., Esposito, R., Steele-MacInnis, M., Hauri,
980 E.H., Wallace, P.J., Plank, T., and Bodnar, R.J. (2015) Bubbles matter: An
981 assessment of the contribution of vapor bubbles to melt inclusion volatile budgets.
982 American Mineralogist, 100(4), 806-823, doi:10.2138/am-2015-5036.
983 Mysen, B. (2014) Water-melt interaction in hydrous magmatic systems at high
984 temperature and pressure. Progress in Earth and Planetary Science, 1(1), 4,
985 doi:10.1186/2197-4284-1-4.
986 Nash, W.P. (1992) Analysis of oxygen with the electron microprobe: Applications to

Always consult and cite the final, published document. See http:/www.minsocam.org or GeoscienceWorld

This is a preprint, the final version is subject to change, of the American Mineralogist (MSA)
Cite as Authors (Year) Title. American Mineralogist, in press.
DOI: https://doi.org/10.2138/am-2019-6735

hydrated glass and minerals. American Mineralogist, 77(3-4), 453-457.

Newman, S., and Lowenstern, J.B. (2002) VolatileCalc: a silicate melt–H_2O–CO_2 solution model written in Visual Basic for excel. Computers & Geosciences, 28(5), 597-604, doi:10.1016/S0098-3004(01)00081-4.

Nowak, M., and Behrens, H. (1995) The speciation of water in haplogranitic glasses and melts determined by in situ near-infrared spectroscopy. Geochimica et Cosmochimica Acta, 59(16), 3445-3450, doi:10.1016/0016-7037(95)00237-T.

Nye, C.J., and Reid, M.R. (1986) Geochemistry of primary and least fractionated lavas from Okmok volcano, Central Aleutians: implications for arc magmagenesis. Journal of Geophysical Research, 91(B10), 10271-10287, doi:10.1029/JB091iB10p10271.

Ochs, F.A., and Lange, R.A. (1999) The Density of Hydrous Magmatic Liquids. Science, 283(5406), 1314-1317, doi:10.1126/science.283.5406.1314.

Ozerov, A.Y. (2000) The evolution of high-alumina basalts of the Klyuchevskoy volcano, Kamchatka, Russia, based on microprobe analyses of mineral inclusions. Journal of Volcanology and Geothermal Research, 95(1–4), 65-79, doi:10.1016/S0377-0273(99)00118-3.

Ozerov, A.Y. (2009) Experimental modeling of the explosion mechanism of basaltic magmas. Petrology, 17(7), 653-668, doi:10.1134/s0869591109070029.

Ozerov, A.Y., Ariskin, A.A., Kyle, P., Bogoyavlenskaya, G.E., and Karpenko, S.F. (1997) Petrological-geochemical model for genetic relationships between basaltic and andesitic magmatism of Klyuchevskoi and Bezymyannyi volcanoes, Kamchatka. Petrology, 5(6), 550-569.

Always consult and cite the final, published document. See http:/www.minsocam.org or GeoscienceWorld

1010 Paonita, A. (2005) Noble gas solubility in silicate melts:a review of experimentation and
1011 theory, and implications regarding magma degassing processes. Annals of
1012 Geophysics, 48(4-5), 647-669, doi:10.4401/ag-3225.
1013 Papale, P., Moretti, R., and Barbato, D. (2006) The compositional dependence of the
1014 saturation surface of H_2O+CO_2 fluids in silicate melts. Chemical Geology, 229(1),
1015 78-95, doi:10.1016/j.chemgeo.2006.01.013.
1016 Parai, R., and Mukhopadhyay, S. (2012) How large is the subducted water flux? New
1017 constraints on mantle regassing rates. Earth and Planetary Science Letters, 317–
1018 318, 396-406, doi:10.1016/j.epsl.2011.11.024.
1019 Peslier, A.H., Schönbächler, M., Busemann, H., and Karato, S.-I. (2017) Water in the
1020 Earth's Interior: Distribution and Origin. Space Science Reviews, 212(1), 743-
1021 810, doi:10.1007/s11214-017-0387-z.
1022 Petrelli, M., El Omari, K., Spina, L., Le Guer, Y., La Spina, G., and Perugini, D. (2018)
1023 Timescales of water accumulation in magmas and implications for short warning
1024 times of explosive eruptions. Nature Communications, 9(1), 770,
1025 doi:10.1038/s41467-018-02987-6.
1026 Plank, T., Kelley, K.A., Zimmer, M.M., Hauri, E.H., and Wallace, P.J. (2013) Why do
1027 mafic arc magmas contain ~4 wt% water on average? Earth and Planetary
1028 Science Letters, 364, 168-179, doi:10.1016/j.epsl.2012.11.044.
1029 Portnyagin, M., Almeev, R., Matveev, S., and Holtz, F. (2008) Experimental evidence for
1030 rapid water exchange between melt inclusions in olivine and host magma. Earth
1031 and Planetary Science Letters, 272(3–4), 541-552,
1032 doi:10.1016/j.epsl.2008.05.020.

Always consult and cite the final, published document. See http:/www.minsocam.org or GeoscienceWorld

This is a preprint, the final version is subject to change, of the American Mineralogist (MSA)
Cite as Authors (Year) Title. American Mineralogist, in press.
DOI: https://doi.org/10.2138/am-2019-6735

1033 Portnyagin, M., Hoernle, K., Plechov, P., Mironov, N., and Khubunaya, S. (2007)
1034 Constraints on mantle melting and composition and nature of slab components in
1035 volcanic arcs from volatiles (H_2O, S, Cl, F) and trace elements in melt inclusions
1036 from the Kamchatka Arc. Earth and Planetary Science Letters, 255(1–2), 53-69,
1037 doi:10.1016/j.epsl.2006.12.005.
1038 Pozgay, S.H., Wiens, D.A., Conder, J.A., Shiobara, H., and Sugioka, H. (2009) Seismic
1039 attenuation tomography of the Mariana subduction system: Implications for
1040 thermal structure, volatile distribution, and slow spreading dynamics.
1041 Geochemistry, Geophysics, Geosystems, 10(4), Q04X05, doi:
1042 10.1029/2008GC002313.
1043 Qin, Z., Lu, F., and Anderson, A.T. (1992) Diffusive reequilibration of melt and fluid
1044 inclusions. American Mineralogist, 77(5-6), 565-576.
1045 Rivalta, E., Taisne, B., Bunger, A.P., and Katz, R.F. (2015) A review of mechanical
1046 models of dike propagation: Schools of thought, results and future directions.
1047 Tectonophysics, 638, 1-42, doi:10.1016/j.tecto.2014.10.003.
1048 Rubin, A.M. (1993) Tensile fracture of rock at high confining pressure: Implications for
1049 dike propagation. Journal of Geophysical Research: Solid Earth, 98(B9), 15919-
1050 15935, doi:doi:10.1029/93JB01391.
1051 Ruprecht, P., and Plank, T. (2013) Feeding andesitic eruptions with a high-speed
1052 connection from the mantle. Nature, 500(7460), 68-72, doi:10.1038/nature12342.
1053 Ruscitto, D.M., Wallace, P.J., and Kent, A.J.R. (2011) Revisiting the compositions and
1054 volatile contents of olivine-hosted melt inclusions from the Mount Shasta region:
1055 implications for the formation of high-Mg andesites. Contributions to Mineralogy

Always consult and cite the final, published document. See http:/www.minsocam.org or GeoscienceWorld

This is a preprint, the final version is subject to change, of the American Mineralogist (MSA)
Cite as Authors (Year) Title. American Mineralogist, in press.
DOI: https://doi.org/10.2138/am-2019-6735

and Petrology, 162(1), 109-132, doi:10.1007/s00410-010-0587-y.

Rutherford, M.J., and Devine, J.D. (1996) Preeruption pressure-temperature conditions and volatiles in the 1991 dacitic magma of Mount Pinatubo. Fire and mud: eruptions and lahars of Mt. Pinatubo, Philippines, p. 751–766. USGS.

Schiano, P. (2003) Primitive mantle magmas recorded as silicate melt inclusions in igneous minerals. Earth-Science Reviews, 63(1), 121-144, doi:10.1016/S0012-8252(03)00034-5.

Schiano, P., and Bourdon, B. (1999) On the preservation of mantle information in ultramafic nodules: glass inclusions within minerals versus interstitial glasses. Earth and Planetary Science Letters, 169(1), 173-188, doi:10.1016/S0012-821X(99)00074-6.

Shishkina, T.A. (2012) Storage conditions and degassing processes of low-K and high-Al tholeiitic island-arc magmas: experimental constraints and natural observations for Mutnovsky volcano, Kamchatka. Naturwissenschaftliche Fakultät, Ph.D., p. 214. Leibniz Universität Hannover, Hannover.

Shishkina, T.A., Botcharnikov, R.E., Holtz, F., Almeev, R.R., Jazwa, A.M., and Jakubiak, A.A. (2014) Compositional and pressure effects on the solubility of H_2O and CO_2 in mafic melts. Chemical Geology, 388, 112-129, doi:10.1016/j.chemgeo.2014.09.001

Shishkina, T.A., Botcharnikov, R.E., Holtz, F., Almeev, R.R., and Portnyagin, M.V. (2010) Solubility of H_2O- and CO_2-bearing fluids in tholeiitic basalts at pressures up to 500 MPa. Chemical Geology, 277(1–2), 115-125, doi:10.1016/j.chemgeo.2010.07.014.

Always consult and cite the final, published document. See http:/www.minsocam.org or GeoscienceWorld

1079 Silver, L., and Stolper, E. (1989) Water in Albitic Glasses. Journal of Petrology, 30(3),
1080 667-709, doi:10.1093/petrology/30.3.667.
1081 Sommer, M.A. (1977) Volatiles H_2O, CO_2, and CO in Silicate Melt Inclusions in Quartz
1082 Phenocrysts from the Rhyolitic Bandelier Air-Fall and Ash-Flow Tuff, New
1083 Mexico. The Journal of Geology, 85(4), 423-432, doi:10.1086/628316.
1084 Steele-Macinnis, M., Esposito, R., and Bodnar, R.J. (2011) Thermodynamic Model for
1085 the Effect of Post-entrapment Crystallization on the H_2O–CO_2 Systematics of
1086 Vapor-saturated, Silicate Melt Inclusions. Journal of Petrology, 52(12), 2461-
1087 2482, doi:10.1093/petrology/egr052.
1088 Steele-MacInnis, M., Esposito, R., Moore, L.R., and Hartley, M.E. (2017)
1089 Heterogeneously entrapped, vapor-rich melt inclusions record pre-eruptive
1090 magmatic volatile contents. Contributions to Mineralogy and Petrology, 172(4),
1091 18, doi:10.1007/s00410-017-1343-3.
1092 Stolper, E. (1982a) The speciation of water in silicate melts. Geochimica et
1093 Cosmochimica Acta, 46(12), 2609-2620, doi:10.1016/0016-7037(82)90381-7.
1094 Stolper, E. (1982b) Water in silicate glasses: An infrared spectroscopic study.
1095 Contributions to Mineralogy and Petrology, 81(1), 1-17, doi:10.1007/bf00371154.
1096 Straub, S.M., LaGatta, A.B., Martin-Del Pozzo, A.L., and Langmuir, C.H. (2008)
1097 Evidence from high-Ni olivines for a hybridized peridotite/pyroxenite source for
1098 orogenic andesites from the central Mexican Volcanic Belt. Geochemistry,
1099 Geophysics, Geosystems, 9(3), Q03007, doi:10.1029/2007GC001583.
1100 Straub, S.M., and Layne, G.D. (2003) The systematics of chlorine, fluorine, and water in
1101 Izu arc front volcanic rocks: Implications for volatile recycling in subduction

Always consult and cite the final, published document. See http:/www.minsocam.org or GeoscienceWorld

zones. Geochimica et Cosmochimica Acta, 67(21), 4179-4203, doi:10.1016/S0016-7037(03)00307-7.

Streck, M.J., and Leeman, W.P. (2018) Petrology of "Mt. Shasta" high-magnesian andesite (HMA): A product of multi-stage crustal assembly. American Mineralogist, 103(2), 216-240, doi:10.2138/am-2018-6151.

Stroncik, N.A., and Schmincke, H.-U. (2002) Palagonite – a review. International Journal of Earth Sciences, 91(4), 680-697, doi:10.1007/s00531-001-0238-7.

Taisne, B., and Jaupart, C. (2011) Magma expansion and fragmentation in a propagating dyke. Earth and Planetary Science Letters, 301(1), 146-152, doi:10.1016/j.epsl.2010.10.038.

Tolstykh, M.L., Naumov, V.B., Gavrilenko, M.G., Ozerov, A.Y., and Kononkova, N.N. (2012) Chemical composition, volatile components, and trace elements in the melts of the Gorely volcanic center, southern Kamchatka: Evidence from inclusions in minerals. Geochemistry International, 50(6), 522-550, doi:10.1134/S0016702912060079.

van Keken, P.E., Hacker, B.R., Syracuse, E.M., and Abers, G.A. (2011) Subduction factory: 4. Depth-dependent flux of H_2O from subducting slabs worldwide. Journal of Geophysical Research: Solid Earth, 116(B1), doi:10.1029/2010JB007922.

Wallace, P.J. (2005) Volatiles in subduction zone magmas: concentrations and fluxes based on melt inclusion and volcanic gas data. Journal of Volcanology and Geothermal Research, 140(1–3), 217-240, doi:10.1016/j.jvolgeores.2004.07.023.

Wallace, P.J., Kamenetsky, V.S., and Cervantes, P. (2015a) Melt inclusion CO_2 contents,

Always consult and cite the final, published document. See http:/www.minsocam.org or GeoscienceWorld

This is a preprint, the final version is subject to change, of the American Mineralogist (MSA)
Cite as Authors (Year) Title. American Mineralogist, in press.
DOI: https://doi.org/10.2138/am-2019-6735

1125 pressures of olivine crystallization, and the problem of shrinkage bubbles.
1126 American Mineralogist, 100(4), 787-794, doi:10.2138/am-2015-5029.
1127 Wallace, P.J., Plank, T., Edmonds, M., and Hauri, E.H. (2015b) Chapter 7 - Volatiles in
1128 Magmas. In H. Sigurdsson, Ed. The Encyclopedia of Volcanoes (Second Edition),
1129 p. 163-183. Academic Press, Amsterdam, doi:10.1016/B978-0-12-385938-
1130 9.00007-9.
1131 Walowski, K., Wallace, P., Cashman, K., Marks, J. K., Clynne, M., Ruprecht, P. (in
1132 review) Understanding melt evolution and eruption dynamics of the 1666 C.E.
1133 eruption of Cinder Cone, Lassen Volcanic National Park, California: Insights
1134 from olivine- hosted melt inclusions. Journal of Volcanology and Geothermal
1135 Research.
1136 Wanamaker, B.J., Wong, T.-F., and Evans, B. (1990) Decrepitation and crack healing of
1137 fluid inclusions in San Carlos olivine. Journal of Geophysical Research: Solid
1138 Earth, 95(B10), 15623-15641, doi:10.1029/JB095iB10p15623.
1139 Weller, D.J., and Stern, C.R. (2018) Along-strike variability of primitive magmas (major
1140 and volatile elements) inferred from olivine-hosted melt inclusions, southernmost
1141 Andean Southern Volcanic Zone, Chile. Lithos, 296-299, 233-244,
1142 doi:10.1016/j.lithos.2017.11.009.
1143 Zellmer, G.F., Edmonds, M., and Straub, S.M. (2015) Volatiles in subduction zone
1144 magmatism. Geological Society, London, Special Publications, 410(1), 1-17,
1145 doi:10.1144/sp410.13.
1146 Zellmer, G.F., Pistone, M., Iizuka, Y., Andrews, B.J., Gómez-Tuena, A., Straub, S.M.,
1147 and Cottrell, E. (2016) Petrogenesis of antecryst-bearing arc basalts from the

Always consult and cite the final, published document. See http:/www.minsocam.org or GeoscienceWorld

Trans-Mexican Volcanic Belt: Insights into along-arc variations in magma-mush ponding depths, H_2O contents, and surface heat flux. American Mineralogist, 101(11), 2405-2422, doi:10.2138/am-2016-5701.

Zhang, H.L., Hirschmann, M.M., Cottrell, E., and Withers, A.C. (2017) Effect of pressure on $Fe^{3+}/\Sigma Fe$ ratio in a mafic magma and consequences for magma ocean redox gradients. Geochimica et Cosmochimica Acta, 204, 83-103, doi:10.1016/j.gca.2017.01.023.

Zhang, Y. (1998) Mechanical and phase equilibria in inclusion–host systems. Earth and Planetary Science Letters, 157(3), 209-222, doi:10.1016/S0012-821X(98)00036-3.

Zimmer, M.M., Plank, T., Hauri, E.H., Yogodzinski, G.M., Stelling, P., Larsen, J., Singer, B., Jicha, B., Mandeville, C., and Nye, C.J. (2010) The Role of Water in Generating the Calc-alkaline Trend: New Volatile Data for Aleutian Magmas and a New Tholeiitic Index. Journal of Petrology, 51(12), 2411-2444, doi:10.1093/petrology/egq062.

Figure Captions

Figure 1. Measured H_2O variations in melt inclusions with different bulk compositions. Major element compositions of the melt inclusions are normalized to an anhydrous basis, and SiO_2 is plotted. H_2O concentrations range up to 8-9 wt% (bold dashed green line). Experimental results showing the maximum possible H_2O content in a mafic glass (this study) are shown with a red circle (1-σ error bars). Quenched glassy melt inclusions have

Always consult and cite the final, published document. See http:/www.minsocam.org or GeoscienceWorld

This is a preprint, the final version is subject to change, of the American Mineralogist (MSA)
Cite as Authors (Year) Title. American Mineralogist, in press.
DOI: https://doi.org/10.2138/am-2019-6735

not been found with high water contents (14-16 wt% of H_2O), which have been suggested by some petrological and geochemical studies (for example, Carmichael 2002; Fischer and Marty 2005; Krawczynski et al. 2012). Dashed grey and blue lines are H_2O solubility limits for 500 MPa having no CO_2 (grey line) and having 2500 ppm of CO_2 provided by the model reported in Shishkina et al. (2014). MI data (6300 analyses) are from the GEOROC database (http://georoc.mpch-mainz.gwdg.de/georoc). The histogram at the bottom panel illustrates the distribution of studied MIs by SiO_2 content showing the abundance of mafic MIs in the global compilation due to numerous studies of primitive magmas.

Figure 2. The variations of cooling rates (green and red thin lines) during quenching of the experiments. The experimental quench rates at the glass transition temperatures (solid circles) are higher than natural cooling rates for MIs in 2 cm lapilli (grey hatching) determined by Lloyd et al. (2013). Glass transition temperatures (solid circles) are calculated for every experimental melt composition using Deubener et al. (2003).

Figure 3. The comparison of natural and experimental temperature drop during quenching. The experimental quench rates (green and red thin lines) are very close to cooling rates of natural glasses (black and blue thick lines). Blue thick lines show the cooling rates of MIs in 2 cm lapilli determined by Lloyd et al. (2013). Black thick lines are modeled cooling rates of glass in pillow lava rims at different depths from the margin reported in Cottrell and Kelley (2011). The model for the depth of 0.5 mm is assumed as

Always consult and cite the final, published document. See http:/www.minsocam.org or GeoscienceWorld

This is a preprint, the final version is subject to change, of the American Mineralogist (MSA)
Cite as Authors (Year) Title. American Mineralogist, in press.
DOI: https://doi.org/10.2138/am-2019-6735

a cooling rate for MIs from in ash particles. The glass transition temperatures (solid circles) are determined as in Figure 2.

Figure 4. H_2O content in products of 1 GPa experiments. Red diamonds show EPMA data, yellow circles – TGA measurements (1-σ error bars). Crossed symbols are from experiments with isobaric quench. Mafic compositions have a limit for incorporation of H_2O in the quenched glass structure, which is significantly lower than H_2O solubility at 1 GPa for basaltic melt (Mitchell et al. 2017). The green line represents the quenchability limit for mafic compositions.

Figure 5. Texture changing with increasing pre-loaded H_2O contents. The amount of preloaded H_2O increases from left to right, in wt%. See text for discussion.

Figure 6. Powder XRD patterns of products from the three experiments. Asterisks (*) indicate a periclase (MgO) contaminant from the experimental assembly. Patterns F091 and F098 have been offset vertically for clarity.

Figure 7. (left) Low-angle region of powder XRD patterns of the experimental products, highlighting phyllosilicate basal reflections. (right) Phyllosilicate (060) features, with the gray band indicating a d-spacing range of 1.525 to 1.545 Å. Patterns F091 and F098 have been offset vertically for clarity.

Always consult and cite the final, published document. See http:/www.minsocam.org or GeoscienceWorld

This is a preprint, the final version is subject to change, of the American Mineralogist (MSA)
Cite as Authors (Year) Title. American Mineralogist, in press.
DOI: https://doi.org/10.2138/am-2019-6735

Figure 8. SEM images of the non-glassy run products – a) F071, b) F091, c) F098, mainly consisting of phyllosilicates (having flaky appearance) – in comparison with the glassy one – d) F099.

Figure 9. Pressure-drop during the quenching period of hydrous experiments at 1 GPa and 1.5 GPa. The pressure for each experiment at the point when it crossed the estimated glass transition temperature was always at least 50-100 MPa above 0.5 GPa which is where ~9 wt% would be the H_2O solubility in a basaltic melt (e.g. Shishkina et al. 2010; Shishkina 2012 and references within). The glass transition temperatures (solid circles) are determined as in Figure 2.

Always consult and cite the final, published document. See http:/www.minsocam.org or GeoscienceWorld

This is a preprint, the final version is subject to change, of the American Mineralogist (MSA)
Cite as Authors (Year) Title. American Mineralogist, in press.
DOI: https://doi.org/10.2138/am-2019-6735

Figure 1.

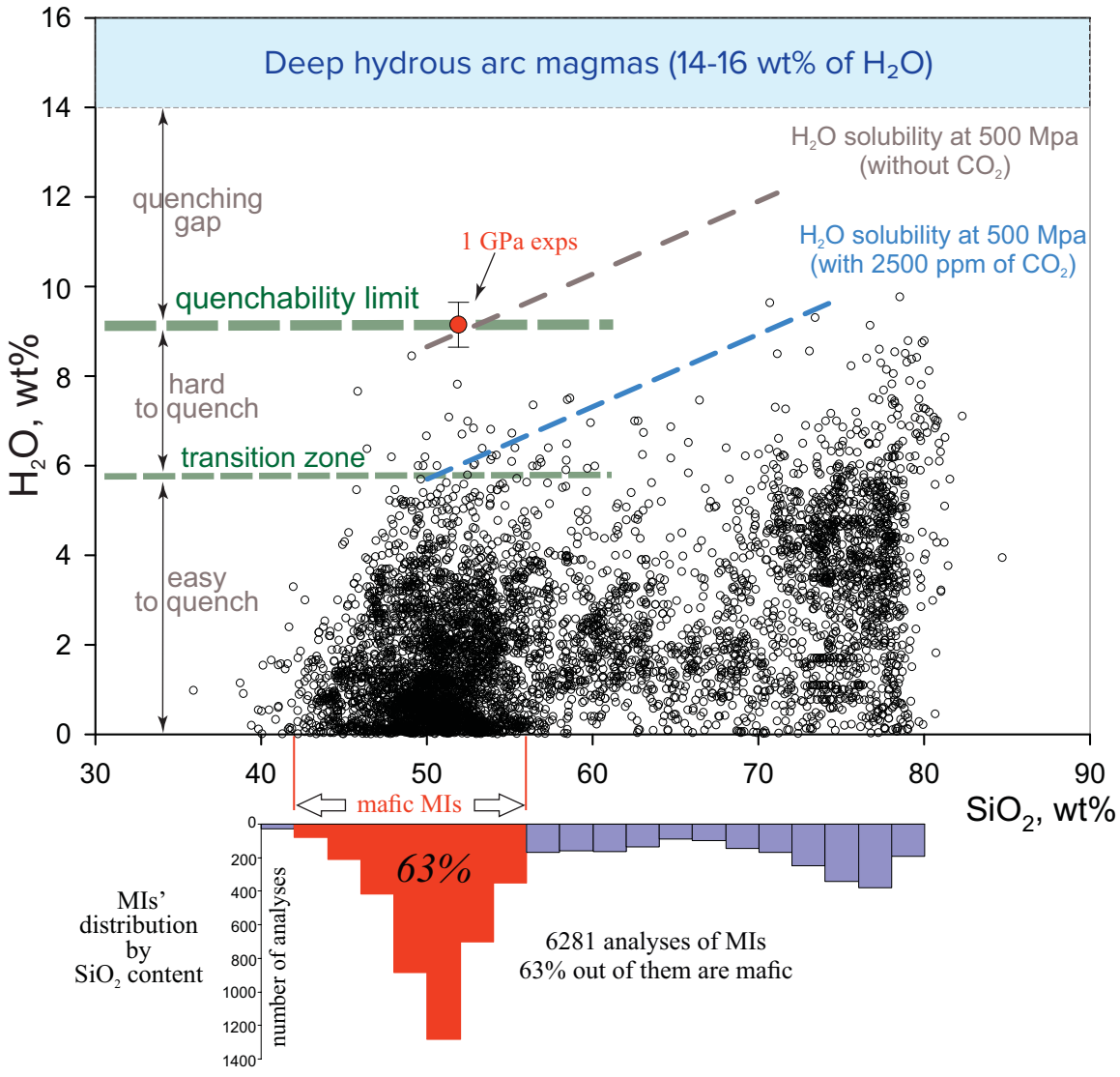

Always consult and cite the final, published document. See http:/www.minsocam.org or GeoscienceWorld

This is a preprint, the final version is subject to change, of the American Mineralogist (MSA)
Cite as Authors (Year) Title. American Mineralogist, in press.
DOI: https://doi.org/10.2138/am-2019-6735

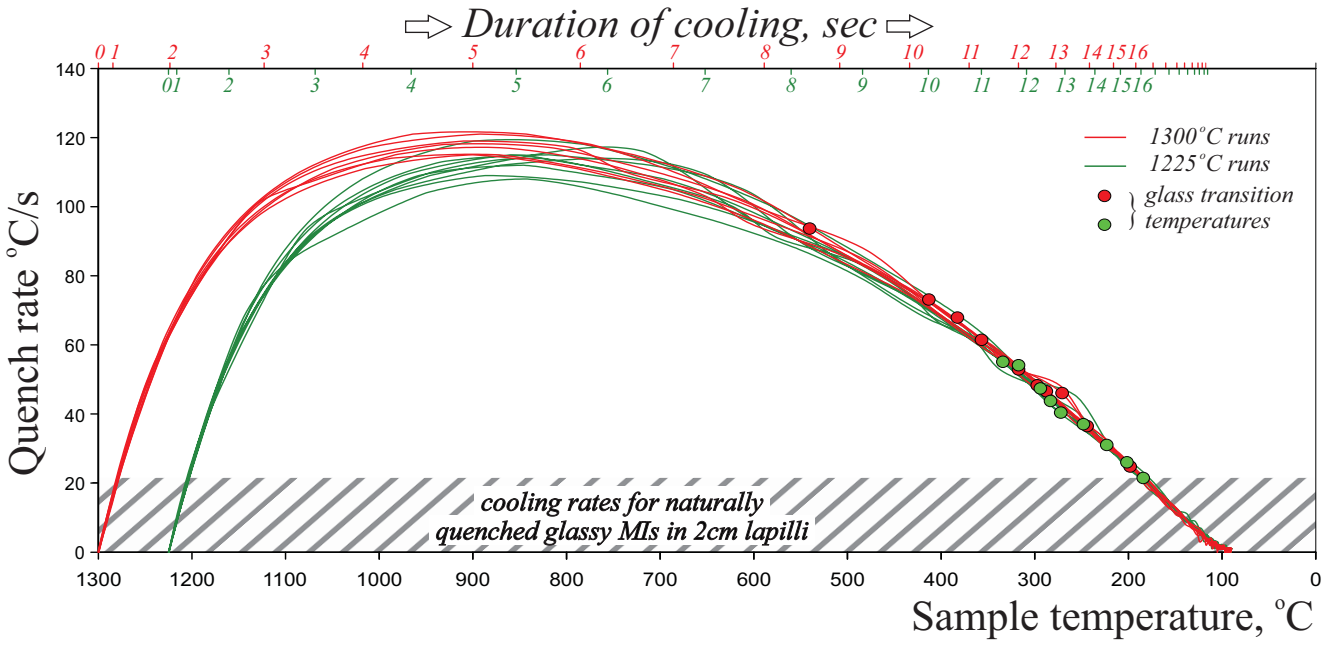

Figure 2.

Always consult and cite the final, published document. See http:/www.minsocam.org or GeoscienceWorld

This is a preprint, the final version is subject to change, of the American Mineralogist (MSA)
Cite as Authors (Year) Title. American Mineralogist, in press.
DOI: https://doi.org/10.2138/am-2019-6735

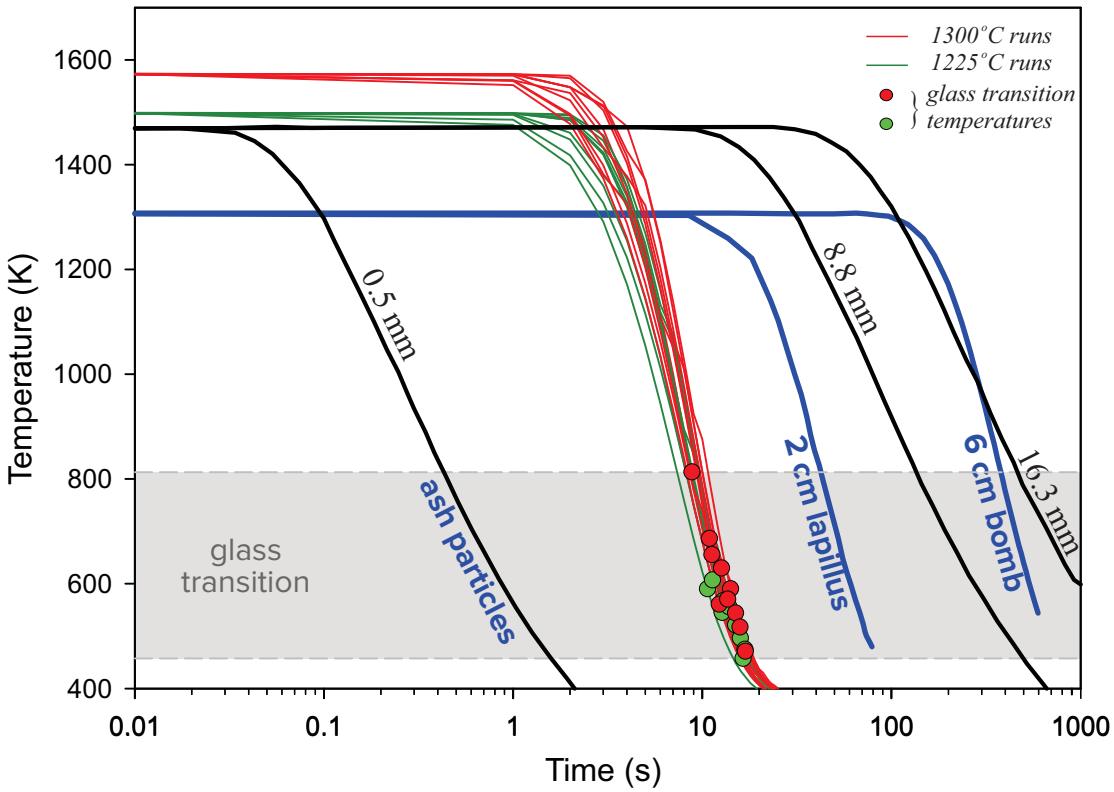

Figure 3.

Always consult and cite the final, published document. See http:/www.minsocam.org or GeoscienceWorld

This is a preprint, the final version is subject to change, of the American Mineralogist (MSA)
Cite as Authors (Year) Title. American Mineralogist, in press.
DOI: https://doi.org/10.2138/am-2019-6735

Figure 4.

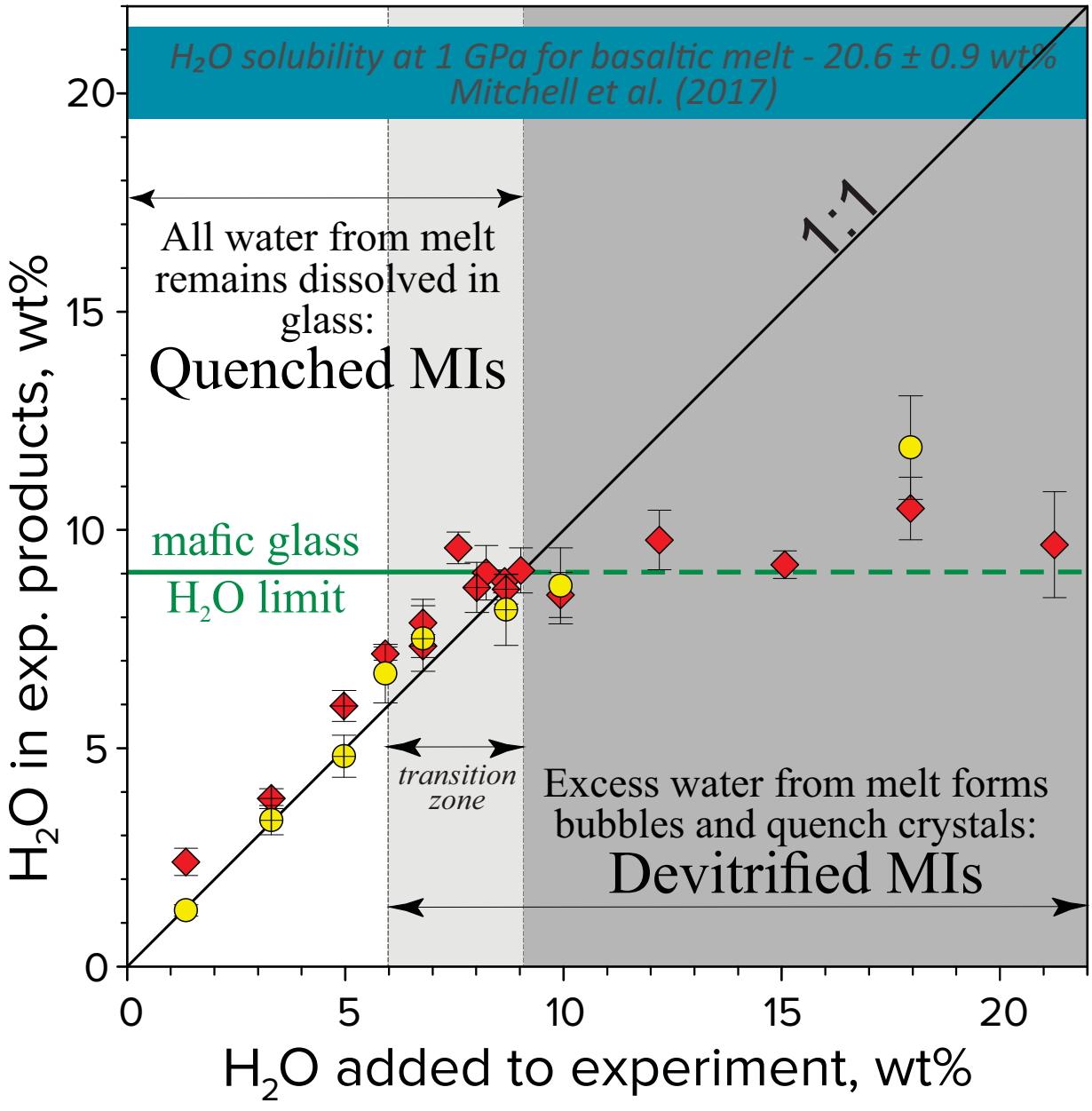

Always consult and cite the final, published document. See http:/www.minsocam.org or GeoscienceWorld

This is a preprint, the final version is subject to change, of the American Mineralogist (MSA)
Cite as Authors (Year) Title. American Mineralogist, in press.
DOI: https://doi.org/10.2138/am-2019-6735

Figure 5.

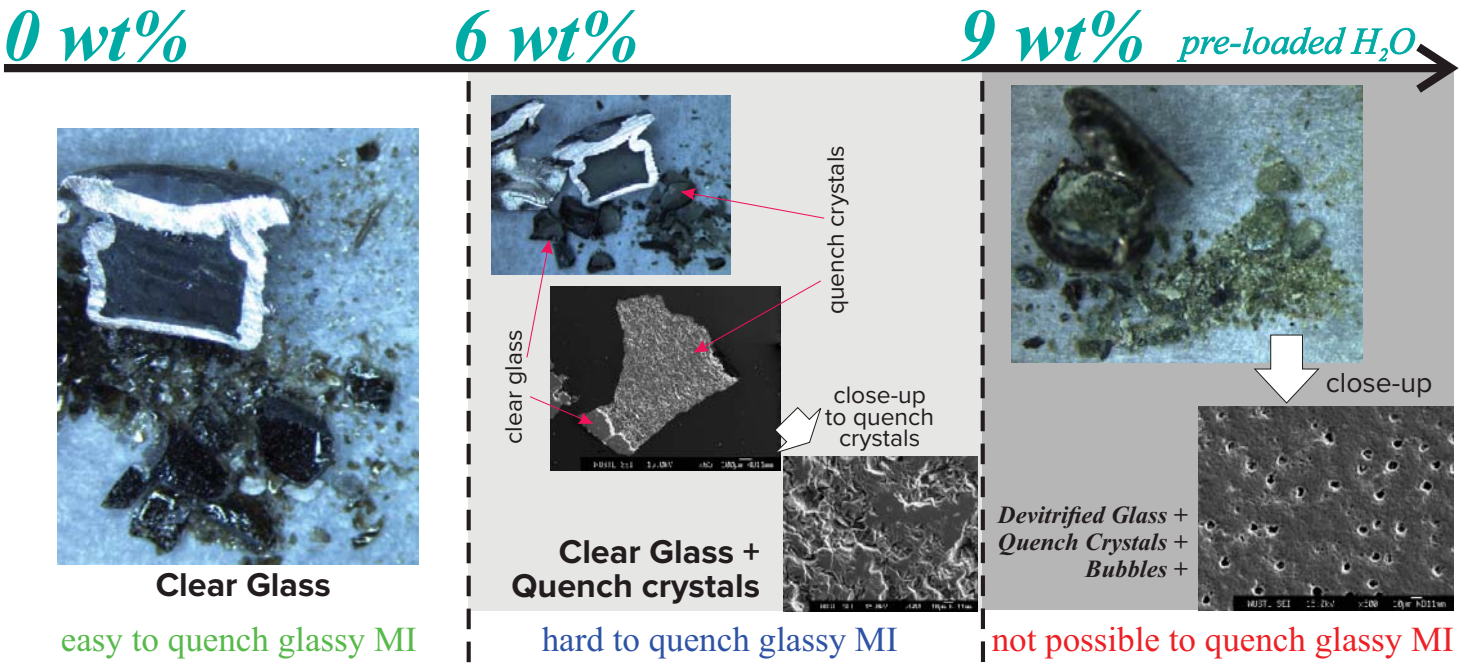

Always consult and cite the final, published document. See http:/www.minsocam.org or GeoscienceWorld

This is a preprint, the final version is subject to change, of the American Mineralogist (MSA)
Cite as Authors (Year) Title. American Mineralogist, in press.
DOI: https://doi.org/10.2138/am-2019-6735

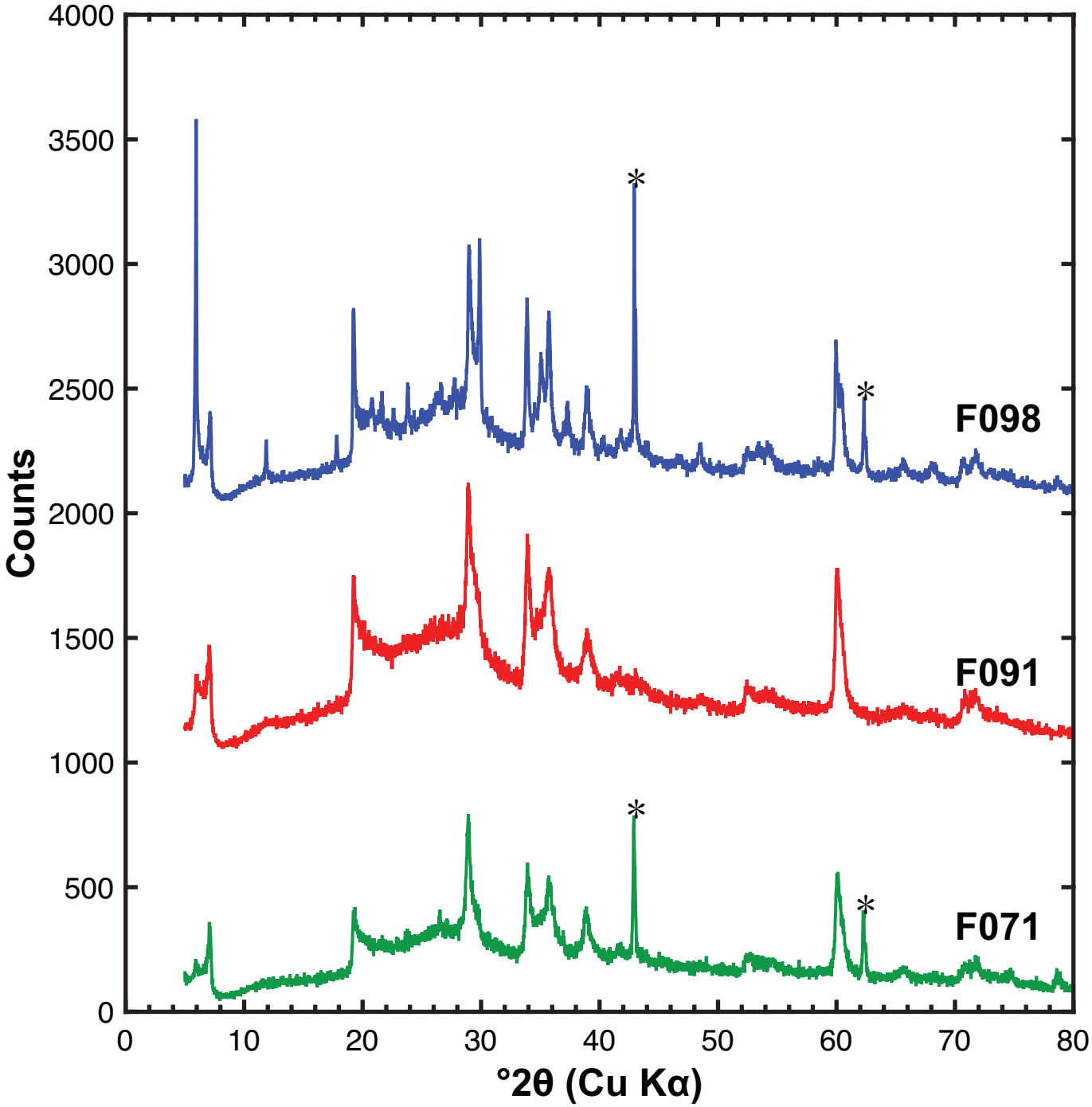

Figure 6.

Always consult and cite the final, published document. See http:/www.minsocam.org or GeoscienceWorld

This is a preprint, the final version is subject to change, of the American Mineralogist (MSA)
Cite as Authors (Year) Title. American Mineralogist, in press.
DOI: https://doi.org/10.2138/am-2019-6735

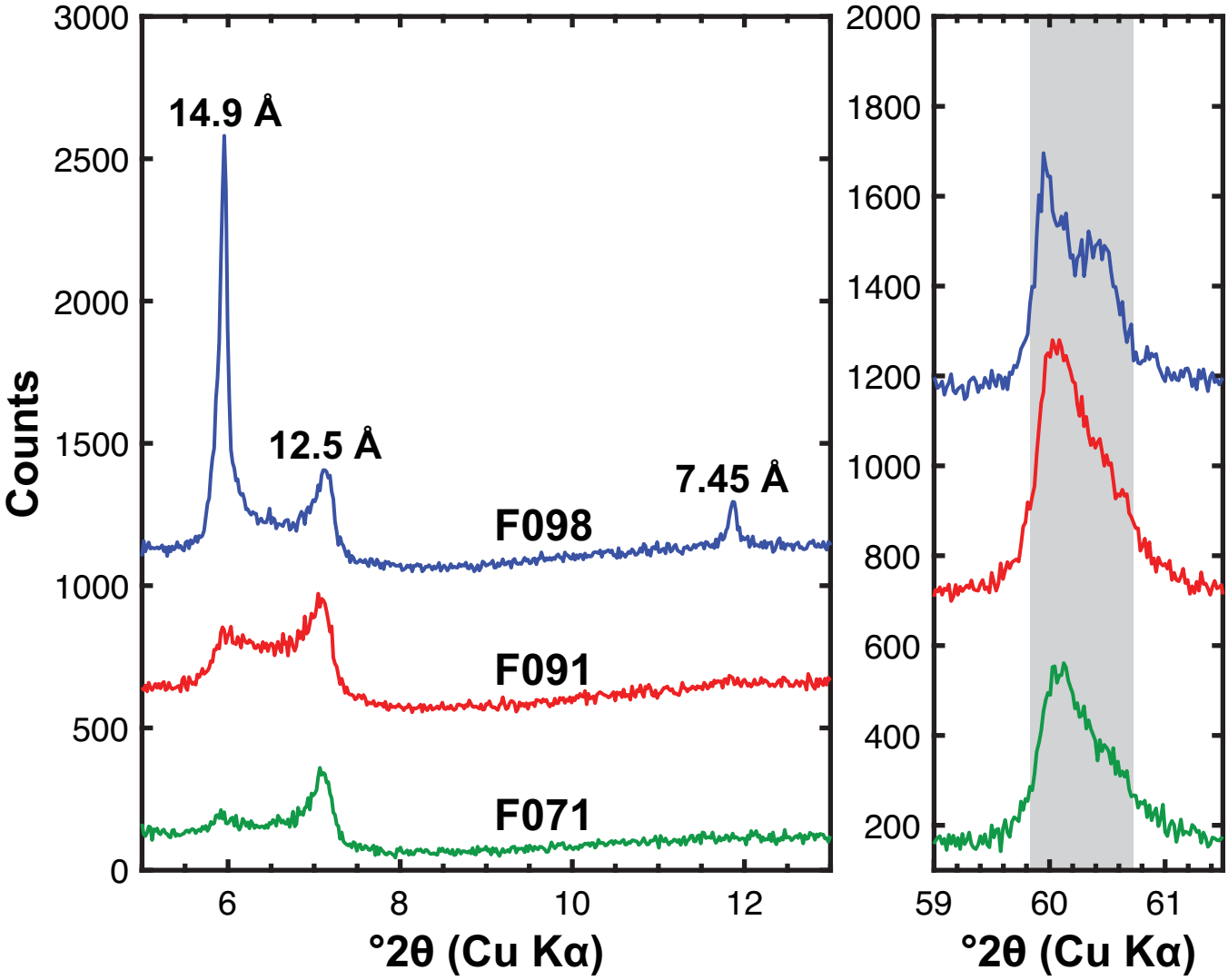

Figure 7.

Always consult and cite the final, published document. See http:/www.minsocam.org or GeoscienceWorld

This is a preprint, the final version is subject to change, of the American Mineralogist (MSA)
Cite as Authors (Year) Title. American Mineralogist, in press.
DOI: https://doi.org/10.2138/am-2019-6735

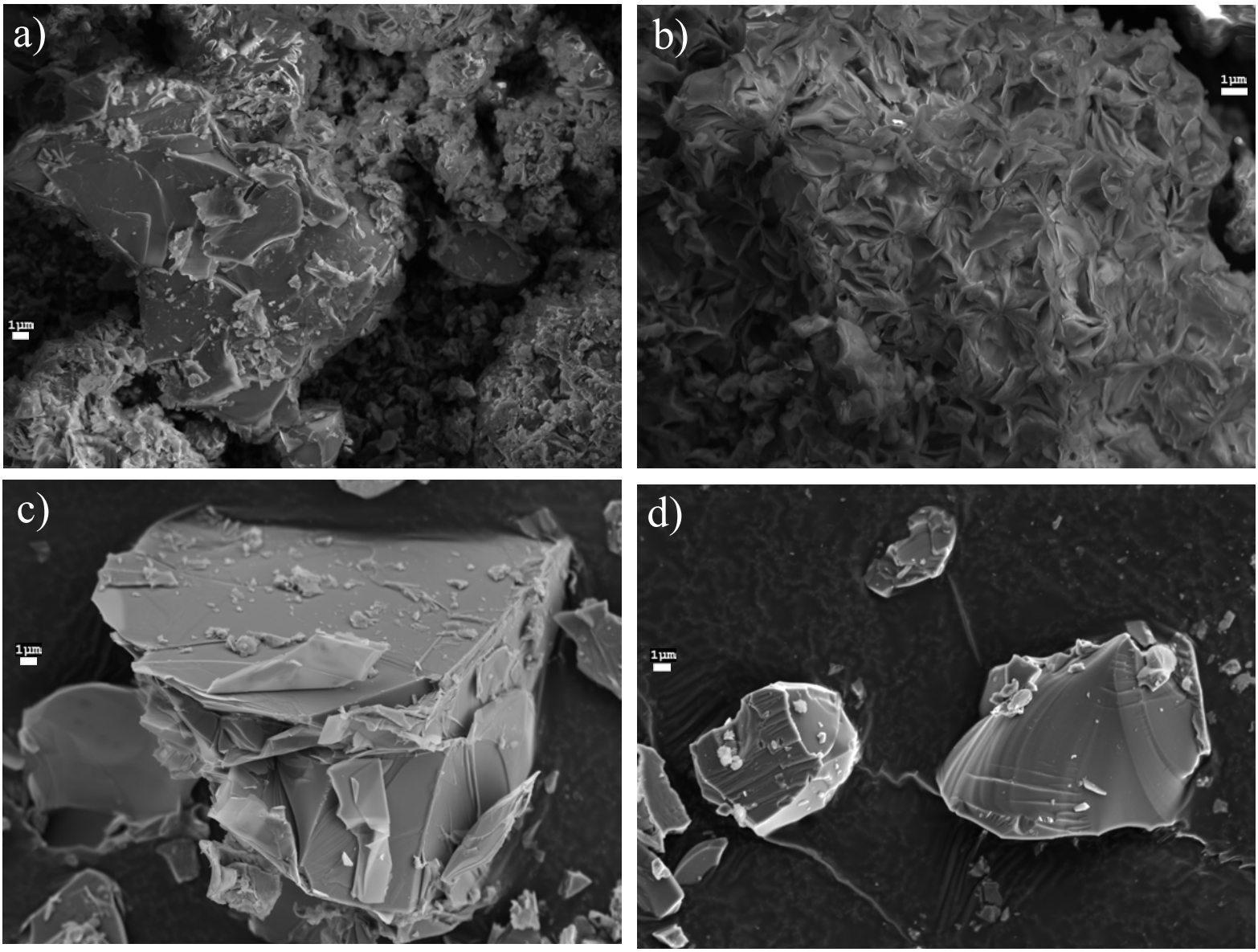

Figure 8.

Always consult and cite the final, published document. See http:/www.minsocam.org or GeoscienceWorld

This is a preprint, the final version is subject to change, of the American Mineralogist (MSA)
Cite as Authors (Year) Title. American Mineralogist, in press.
DOI: https://doi.org/10.2138/am-2019-6735

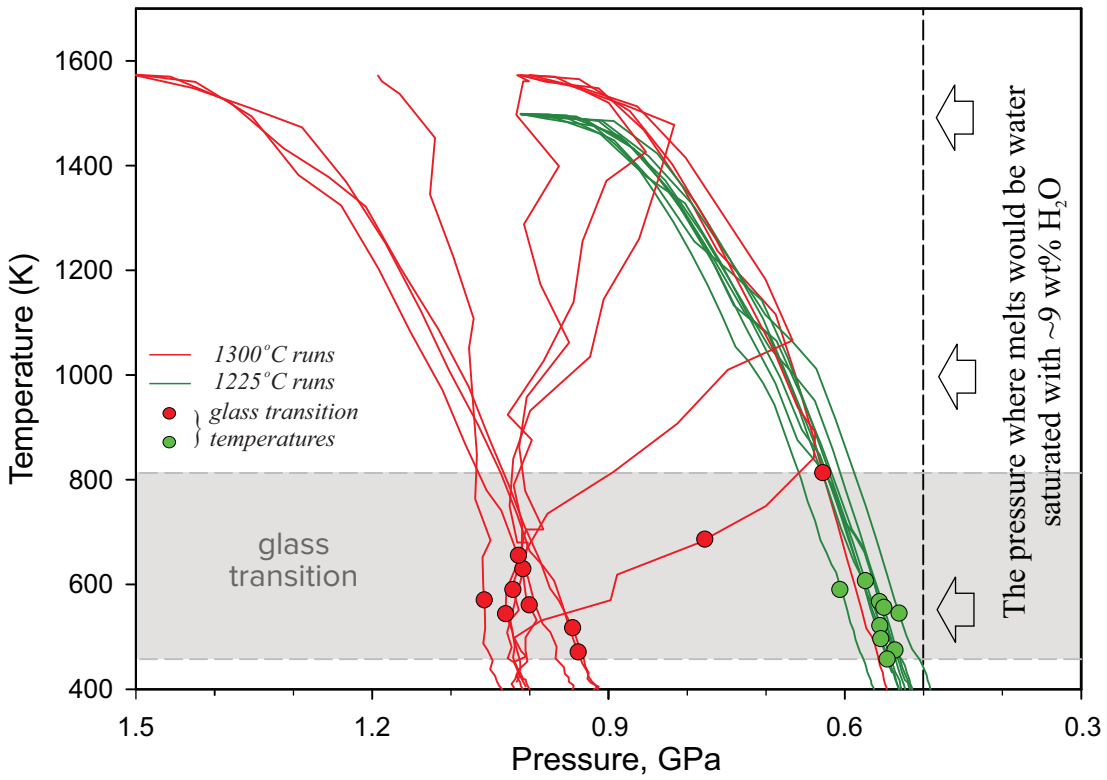

Figure 9.

Always consult and cite the final, published document. See http:/www.minsocam.org or GeoscienceWorld

This is a preprint, the final version is subject to change, of the American Mineralogist (MSA)
Cite as Authors (Year) Title. American Mineralogist, in press.
DOI: https://doi.org/10.2138/am-2019-6735

Table 1. Glass starting material for experiments in oxide weight percents measured by EPMA.

Starting material	n	SiO_2 [a]		TiO_2		Al_2O_3		FeO		MnO		MgO		CaO		Na_2O		K_2O		Total	Mg#
mafic (85-44)	40	51.12	0.85	0.61	0.03	16.58	0.18	7.84	0.24	0.059	0.015	10.43	0.14	9.28	0.08	2.24	0.06	0.39	0.02	98.55	70.3

n - number of probe analyses.
[a] Columns directly following the oxide wt% are 2-σ errors (standard deviation) from replicate analyses.

Always consult and cite the final, published document. See http:/www.minsocam.org or GeoscienceWorld

This is a preprint, the final version is subject to change, of the American Mineralogist (MSA)
Cite as Authors (Year) Title. American Mineralogist, in press.
DOI: https://doi.org/10.2138/am-2019-6735

Table 2. Run conditions and products for hydrous supra-liquidus experiments for 85-44 composition.

Run	Temp., °C	Pressure, GPa	pre-loaded H_2O, wt.%	Duration, hours	Phases[a]	% ΔFe[b]	Tg, °C
F068	1225	1.0	8.7	16	vesicular glass and QC (96) + olivine (4)	-8.4	288
F069	1225	1.0	12.2	16	vesicular glass, QC, and alteration products	-5.6	248
F070	1225	1.0	15.1	16	vesicular glass, QC, and alteration products	-2.9	223
F071	1225	1.0	18.0	14	vesicular glass, QC, and alteration products	-2.9	202
F073	1225	1.0	8.2	16	vesicular glass, QC, and alteration products	-1.2	294
F074	1225	1.0	9.9	16	vesicular glass, QC, and alteration products	-0.6	272
F075	1225	1.0	7.6	16	glass, vesicular glass, QC, and alteration products	0.0	304
F076	1225	1.0	6.8	16	glass (94), QC, + olivine (6)	1.9	317
F079	1225	1.0	5.9	16	glass and rare QC	-1.1	334
F080	1225	1.0	9.0	16	vesicular glass, QC, and alteration products	-0.7	283
F083	1225	1.0	21.3	16	vesicular glass, QC, and alteration products	0.4	184
F085	1300	1.0	1.3	10	glass (88) + pyroxene (12)	-1.4	540
F087	1300	1.0p	3.3	10	glass (?) + pyroxene (?)	1.4	413
F088	1300	1.0p	5.0	10	glass	0.8	357
F089	1300	1.0p	6.8	10	glass + QC	0.7	317
F090	1300	1.0p	8.7	10	vesicular glass, QC, and alteration products	3.1	288
F091	1300	1.0p	10.0	10	vesicular glass, QC, and alteration products		271
F097	1300	1.5	18.5	10	vesicular glass, QC, and alteration products	-3.9	198
F098	1300	1.5	12.6	10	vesicular glass, QC, and alteration products	-2.1	244
F099	1300	1.5	4.1	10	glass (?) + pyroxene (?)	2.4	383
F106	1300	1.0p	8.0	10	glass, QC, and alteration products	-1.6	297
F107	1300	1.0p	12.2	10	vesicular glass, QC, and alteration products		248

[a] in parentheses phases abundances in percent, calculated by mass balance.

[b] percent of relative Fe loss or gain from the starting material based on the difference between the starting material and calculated bulk composition of experiment using a linear regression mass balance.

"1.0p" - **p** means that pressure was maintained during quenching due to active pumping.

Tg - calculated the glass transition temperature based on pre-loaded H_2O content and algorithm from Deubener et al. (2003).

Always consult and cite the final, published document. See http:/www.minsocam.org or GeoscienceWorld

This is a preprint, the final version is subject to change, of the American Mineralogist (MSA)
Cite as Authors (Year) Title. American Mineralogist, in press.
DOI: https://doi.org/10.2138/am-2019-6735

Table 3. EPMA and TGA analyses of experimental run products in oxide weight percent.

Run	Phase	n	SiO_2 [a]		TiO_2		Al_2O_3		FeO		MnO		MgO		CaO		Na_2O		K_2O		Total	pre-loaded H_2O, wt.%	measured H_2O, wt%		
																							by-difference[a]		TGA
F068	BBQM	47	47.69	1.10	0.57	0.04	17.07	0.57	6.50	0.27	0.05	0.02	8.18	0.26	9.08	0.33	1.52	0.26	0.52	0.10	91.18	8.65	8.81	0.52	
	olivine	23	40.63	0.46	0.01	0.02	0.02	0.03	11.24	0.32	0.07	0.02	47.83	0.66	0.12	0.03	0.00	0.01	0.00	0.01	99.93				
F069	BBQM	16	47.15	0.73	0.55	0.05	16.34	0.27	6.77	0.21	0.06	0.02	9.26	0.19	8.58	0.44	1.23	0.52	0.30	0.17	90.23	12.20	9.76	1.37	
F070	BBQM	32	47.28	0.64	0.56	0.04	16.76	0.56	6.94	0.23	0.05	0.02	8.48	0.18	8.81	0.28	1.45	0.26	0.46	0.15	90.79	15.07	9.20	0.63	
F071	BBQM	38	46.01	1.13	0.57	0.03	15.10	0.35	6.89	0.38	0.05	0.02	9.37	0.54	8.70	0.75	2.47	0.87	0.35	0.13	89.50	17.96	10.49	1.44	11.88
F073	glass	30	47.41	0.83	0.56	0.04	15.74	0.13	7.17	0.34	0.05	0.02	9.33	0.39	8.57	0.19	1.70	0.35	0.45	0.07	90.98	8.23	9.01	1.25	
F074	BBQM	30	46.86	1.10	0.57	0.04	16.03	0.38	7.23	0.39	0.06	0.03	9.65	0.48	8.74	0.21	1.85	0.33	0.48	0.09	91.48	9.93	8.51	1.03	8.71
F075	glass	20	47.15	0.75	0.57	0.05	15.84	0.11	7.18	0.46	0.05	0.02	8.85	0.46	8.62	0.25	1.69	0.10	0.45	0.04	90.41	7.59	9.59	0.72	
F076	glass	25	48.20	1.05	0.60	0.03	16.38	0.30	7.47	0.32	0.05	0.02	7.66	0.61	9.31	0.37	2.07	0.21	0.39	0.06	92.12	6.78	7.87	1.08	
	olivine	8	41.11	0.53	0.00	0.01	0.03	0.01	9.06	1.11	0.06	0.02	50.37	0.82	0.11	0.02	0.00	0.01	0.01	0.01	100.75				
F079	glass	30	47.98	0.76	0.57	0.04	15.58	0.24	7.55	0.45	0.06	0.02	9.91	0.42	8.79	0.23	2.02	0.17	0.36	0.04	92.83	5.92	7.16	0.30	6.70
F080	BBQM	26	47.41	0.82	0.55	0.04	15.49	0.73	7.25	0.25	0.05	0.02	9.40	0.80	8.68	0.25	1.70	0.13	0.39	0.05	90.92	9.03	9.07	1.03	
F083	BBQM	23	46.61	1.22	0.55	0.04	15.29	0.42	7.14	0.18	0.05	0.02	9.44	0.33	8.78	0.57	2.01	0.71	0.46	0.15	90.33	21.25	9.66	2.43	
F085	glass	16	50.79	0.66	0.65	0.04	17.45	0.43	7.69	0.34	0.06	0.03	7.94	0.62	10.06	0.18	2.53	0.07	0.43	0.02	97.61	1.35	2.39	0.62	1.28
	pyroxene	10	52.92	1.15	0.10	0.03	6.15	0.89	7.62	0.41	0.06	0.02	31.19	0.58	1.67	0.13	0.06	0.02	0.01	0.01	99.77				
F087	glass	20	50.16	0.96	0.59	0.04	16.19	0.15	7.76	0.58	0.06	0.03	9.67	0.30	9.19	0.29	2.16	0.12	0.37	0.03	96.15	3.31	3.84	0.46	3.34
F088	glass	20	49.05	0.75	0.58	0.04	15.75	0.21	7.54	0.25	0.05	0.03	9.67	0.31	8.91	0.14	2.10	0.07	0.36	0.03	94.03	4.97	5.96	0.71	4.81
F089	glass	20	48.47	0.64	0.56	0.04	15.47	0.31	7.42	0.59	0.05	0.02	9.55	0.61	8.75	0.31	2.01	0.27	0.35	0.04	92.65	6.78	7.33	0.53	7.51
F090	BBQM	25	47.62	1.02	0.57	0.03	15.32	0.29	7.49	0.55	0.05	0.03	9.44	0.58	8.86	0.24	1.54	0.17	0.46	0.06	91.35	8.68	8.64	0.68	8.17
F097	BBQM	14	45.75	0.86	0.55	0.05	14.85	0.31	6.70	0.45	0.05	0.03	9.09	0.74	9.03	0.44	1.35	0.22	0.22	0.06	87.58	18.47	12.38	1.03	
F098	BBQM	14	46.04	1.30	0.53	0.03	14.99	0.42	6.81	0.26	0.04	0.03	8.48	0.50	8.69	0.48	1.56	0.42	0.34	0.20	87.48	12.63	12.50	1.88	
F099	glass	16	48.78	0.91	0.61	0.05	16.37	0.21	7.68	0.50	0.04	0.03	8.96	0.37	9.22	0.34	2.19	0.14	0.38	0.04	94.23	4.11	5.75	0.79	4.40
F106	glass	15	47.99	0.93	0.57	0.05	15.55	0.27	7.15	0.43	0.04	0.03	9.33	0.69	8.60	0.33	1.72	0.17	0.36	0.05	91.31	8.01	8.68	1.15	

n - number of probe analyses.

[a] Columns directly following the oxide wt.% are 2-σ errors (standard deviation) from replicate analyses.

"**BBQM**" refers to 'broad beam analysis of quench-material'

Always consult and cite the final, published document. See http:/www.minsocam.org or GeoscienceWorld

This is a preprint, the final version is subject to change, of the American Mineralogist (MSA)
Cite as Authors (Year) Title. American Mineralogist, in press.
DOI: https://doi.org/10.2138/am-2019-6735

Table 4: Volatile element concentrations determined by secondary ion mass spectrometry

Sample[$]		H_2O (wt.%)	2SD	CO_2 (ppm)	2SD	F (ppm)	2SD	P (ppm)	2SD	S (ppm)	2SD	Cl (ppm)	2SD
F099	n=3	3.93	0.42	575	41	29	3.2	74	1.9	66	0.8	33	1.0
F087	n=3	2.53	0.11	461	21	24	1	68	2	156	7	27	1
MR:ND-70-01[a]	n=11	1.06	0.04			120	6.2	374	6.4	913	22.3	246	13.2
FR:ND-60-01[b]	n=10	1.41	0.04			154	6.9	445	5.4	43	0.6	872	29.7
Suprasil[c]	n=7	0.0029	0.0009			14	4.2	0.8	1.1	5.3	5.0	1100	135

a Preferred values for MR:ND-70-01 are 1.0 wt.% H2O, 80 ppm CO_2, 150 ppm F, 382 ppm P, 888 ppm S, 198 ppm Cl.
No CO_2 concentrations calculated, because this glass was used for calibration.

b Preferred values for FR:ND-60-01 are 1.42 wt.% H2O, 2.7 ppm CO_2, 208 ppm F, 461 ppm P, 42.1 ppm S, 720 ppm Cl.
No CO_2 concentrations calculated, because this glass was used for calibration.

c Suprasil provides estimates for limits of detection for all elements except CO_2 (high background) and Cl (high co**ncentration)**

$ Calibration curves (except for CO_2) used ALV-519-4-1, ALV-1833-11, ALV-1846-12, ALV-1833-1.

Always consult and cite the final, published document. See http:/www.minsocam.org or GeoscienceWorld